VORTEX DYNAMICS IN DOMAINS WITH BOUNDARIES

A Thesis Submitted to
the Graduate School of Engineering and Sciences of
İzmir Institute of Technology
in Partial Fulfillment of the Requirements for the Degree of

DOCTOR OF PHILOSOPHY

in Mathematics

by
Serdar TÜLÜ

June 2011
İZMİR

We approve the thesis of **Serdar TÜLÜ**

_____

Prof. Dr. Oğuz YILMAZ
Supervisor

_____

Prof. Dr. Oktay PASHAEV
Committee Member

_____

Prof. Dr. Can Fuat DELALE
Committee Member

_____

Prof. Dr. İsmail Hakkı DURU
Committee Member

_____

Assoc. Prof. Dr. Ali İhsan NESLİTÜRK
Committee Member

16 June 2011

_____   _____

Prof. Dr. Oğuz YILMAZ   **Prof. Dr. Durmuş Ali DEMİR**
Head of the Department of   Dean of the Graduate School of
Mathematics   Engineering and Sciences

ACKNOWLEDGMENTS

ABSTRACT

VORTEX DYNAMICS IN DOMAINS WITH BOUNDARIES

In this thesis we consider the following problems: 1) The problem of fluid advection excited by point vortices in the presence of stationary cylinders (we also add a uniform flow to the systems). 2) The problem of motion of one vortex (or vortices) around cylinder(s). We also investigate integrable and chaotic cases of motion of two vortices around an oscillating cylinder in the presence of a uniform flow.

In the fluid advection problems Milne-Thomson's Circle theorem and an analytical-numerical solution in the form of an infinite power series are used to determine flow fields and the forces on the cylinder(s) are calculated by the Blasius theorem. In the "two vortices-one cylinder" case we generalize the problem by adding independent circulation κ_0 around the cylinder itself. We then write the conditions for force to be zero on the cylinder.

The Hamiltonian for motion of two vortices in the case with no uniform flow and stationary cylinder is constructed and reduced. Also constant Hamiltonian (energy) curves are plotted when the system is shown to be integrable according to Liouville's definition. By adding uniform flow to the system and by allowing the cylinder to vibrate, we model the natural vibration of the cylinder in the flow field, which has applications in ocean engineering involving tethers or pipelines in a flow field. We conclude that in the chaotic case, forces on the cylinder may be considerably larger than those on the integrable case depending on the initial positions of the vortices, and that complex phenomena such as chaotic capture and escape occur when the initial positions lie in a certain region.

ÖZET

SINIRLARI OLAN BÖLGELERDE GİRDAP DİNAMİĞİ

Bu tezde ele alınan problemler şu şekilde özetlenebilir: 1) Noktasal girdapların sabit silindirlerle birlikte oluşturduğu akışkan hareketi problemi (ayrıca sisteme sabit hızdaki akışkan da eklenerek incelenmektedir). 2) Bir ya da birden fazla girdabın, silindirler etrafındaki hareketleri. Ayrıca sabit hızdaki akışkan içinde bulunan titreşimli bir silindirin etrafındaki iki girdabın integrallenebilir durumdaki ve kaos içindeki girdap hareketleri araştırılmaktadır.

Akışkan hareketi problemlerinde, akışkanın hız alanları, Milne-Thomson'un Daire teoremi, ve analitik ve sayısal formda sonsuz seri çözümleri kullanılarak elde edilmiştir. Blasius teoremi kullanılarak da silindirler üstündeki kuvvetler hesaplanmıştır. "İki girdap - bir silindir" problemi, silindir etrafında bağımsız dolaşım eklenerek genişletilmiş ve silindir üstündeki kuvvetin sıfır olduğu durumlar bulunmuştur.

Durağan akışkan ve silindir olduğunda girdap hareketinin Liouville tanımına göre integrallenebilir olduğu gösterilirken sistemin Hamiltoniyenleri kurulup indirgenmiştir. Ayrıca sabit Hamilton eğrileri çizilmiştir. Sisteme sabit akım ekleyerek ve silindire de titreşim vererek, boru hatlarını ve bağlantıları içeren okyanus mühendisliğinde uygulamaları olan doğal silindir titreşimi modellenmiştir. Kaotik durumlarda silindire uygulanan kuvvetlerin, girdapların başlangıç konumlarına bağlı olarak, integrallenebilir sistemlerden daha büyük olduğu gösterilmiş ve girdapların, başlangıç konumları belirli bir bölgede mevcut olduklarında, bu girdapların kaçışları ve yakalanışları gösterilmiştir.

TABLE OF CONTENTS

LIST OF FIGURES

CHAPTER 1

INTRODUCTION

1.1. Literature Review

The investigation of point vortices in domains with boundaries is a popular research area with possible applications in engineering and physics such as the interaction of tension leg platforms or semisubmersibles with vortices in a uniform flow field. The concept of point vortex motion, a classical model in the theory of two dimensional, incompressible fluid mechanics, was introduced by Helmholtz in 1858. He set down the basic laws of vortex dynamics. The simplest example of the motion of two vortices was considered in (Helmholtz, 1858). Kirchhoff established the Hamiltonian property of the equations of motion of N point vortices, and also found the four first integrals of this system that are related to the time independence of the Hamiltonian and its invariance under parallel translation and rotation of the coordinate frame (Kirchhoff, 1883). The integrability of the problem of three vortices was noted in (Poincare, 1893) (there are three first integrals in involution) and was shown in unbounded plane in (Aref 1983). The analytic proof of the non-integrability of the set of four point vortices on a plane was given in (Ziglin 1980, 1983). He considered the restricted problem of four vortices, that is, three unit vortices and a fourth vortex with zero intensity (i.e., a simple particle of fluid). The system of three identical vortices was integrated in (Aref & Pomphrey 1982) in terms of elliptic functions and it was shown that the motion of four vortices of equal strength is chaotic. In unbounded plane, the integrability of motion of four vortices was shown in (Aref & Pomphrey 1982) and (Eckhardt 1988) for special arrangements of vortices. Integrable cases of the motion of four vortices were examined in (Eckhardt 1988) using the Poisson brackets between constants of motion.

Vortices in annular regions have also been investigated by many authors. Johnson & McDonald solved the problem in terms of elliptic functions (Johnson & McDonald 2005). Analysis of the same problem by the method of images in terms of the q-calculus has been examined in (Pashaev & Yilmaz 2008). Advection problem of a point vortex in closed domains has been studied by Zannetti & Franzese. They use canonical transformations to eliminate the time dependence of the Hamiltonian (Zannetti & Franzese 1993).

In this thesis we consider two different problems: The problem of fluid advection excited by M vortices and a uniform flow in the presence of N stationary cylinders, starting with the simplest case (one vortex and single cylinder), and the problem of motion of the vortices around the cylinders, starting with the case of one vortex and single cylinder.

In the fluid advection problems Milne-Thomson's Circle theorem (Milne-Thomson 1968) is used to determine the flow field for the cases with one cylinder. Further an analytical-numerical solution in the form of an infinite power series for the velocity field is obtained using complex analysis for the cases with N stationary cylinders (Pashaev & Yilmaz 2009). In the fluid advection problem forces are calculated by the Blasius theorem. The Hamiltonian for vortex motion is constructed for all cases.

We investigate integrable and chaotic cases of vortex motion. In dynamical systems, integrability is not usual. Most of the actual problems of dynamics (say, the n-body problem) turns out to be non-integrable. Even if the system is integrable, it is not an easy task to reduce the system to lower space dimensions. In the case of a stationary cylinder and two vortices, we see that the motion of vortices is integrable when the vortices have equal strength. This system is reduced to two space dimensions and constant Hamiltonian (energy) curves are plotted when the system is shown to be integrable according to Liouville's definition. If a uniform flow is added to the system of two vortices and a cylinder, the symmetry is destroyed by the uniform flow and the motion of vortices is probably not integrable.

The last case we consider involves the oscillatory perturbation of the cylinder, uniform flow and vortices. By adding uniform flow to the system, and by allowing the cylinder to vibrate, we model the natural vibration of the cylinder in the flow field, which has applications in ocean engineering involving vortex induced oscillations of tethers or pipelines in a flow field. We demonstrate that chaos exist for certain parameter values and this results in higher forces exerted by the fluid on the cylinder. So, chaotic motion of vortices is not only interesting in its own right, but also it has some practical consequences such as causing increase in forces acting on the cylinder. Chaotic interaction of a cylinder with one vortex has been studied in (Kadtke & Novikov 1993). They show the chaotic capture and escape of vortex and gave a capture zone, shown in Figure 12 of their paper, which is closely related to the separatrix. In our study, in the case of two vortices with a cylinder, a capture zone plot similar to the one given by Kadtke and Novikov is given.

In most vortex induced vibration problems (Banik & Datta 2009) - (Dong, Xie & Lou 1992), numerical and semi analytical techniques have been used to estimate stability, modes of oscillations, displacement and vortex forces. The hydrodynamic interaction

between vortices and an oscillating cylinder in the presence of a uniform flow will be considered, This may be used in understanding vortex induced vibration problems.

Hydrodynamic interaction problem has been studied by many authors in connection with free surface waves and surface piercing vertical cylinders. For example, see (Linton & Evans 1990) and (Yilmaz 1998). The basic idea behind these studies is that, incoming waves can be decomposed into modes and diffracted waves from cylinders can be related to these modes. Then, the interaction takes place when we relate the coordinate systems at the centre of each cylinder by using addition theorems. A similar idea was used by Pashaev and Yilmaz to find the interaction between cylinders and a vortex in the two dimensional plane (Pashaev & Yilmaz 2009). There are other methods such as Abelian function theory and conformal mapping techniques used in solving vortex body interaction problems. For these methods, see (Pashaev & Yilmaz 2008) and (Crowdy & Marshall 2005).

1.2. Structure of the Thesis

In Chapter 2, the fundamentals of two dimensional fluid flow are given. We formulate the problem of fluid advection excited by M vortices and a uniform flow in the presence of N stationary cylinders. The formulas for the forces on the cylinders are given by the Blasius Theorem and we generalize the problem by adding independent circulation around the cylinder.

In Chapter 3, Hamiltonian description of motion of vortices is given. The Hamiltonian for the motion of vortices is constructed. We investigate integrable and chaotic cases of vortex motion. We find an integrable system of two vortices. This system is shown to be integrable according to Liouville's definition, and we reduce it to two space dimensions and plot the constant Hamiltonian curves.

In Chapter 4, we add an oscillatory perturbation to the cylinder of the system of two vortices and a cylinder in the presence of uniform flow. Interesting cases of chaotic capture and escape are shown. Magnitude of the force on the cylinder in the integrable case of two vortices is compared with the non-integrable case.

In conclusions we summarize the main results in the thesis which were published in the paper of "Motion of vortices outside a cylinder", (Tülü & Yilmaz 2010).

CHAPTER 2

FLOW INDUCED BY VORTICES

We consider problems of line vortices and infinitely long cylinders. Hence, the problem can be reduced to the two-dimensional problem of point vortices and discs. Then we shall frequently make use of the theory of complex analytic functions. Complex velocity is defined as

$$\overline{V}(z) = u(x,y) - iv(x,y), \quad z = x + iy, \tag{2.1}$$

where u and v are the velocity components in the $x-$ and $y-$directions, respectively. We assume the flow is incompressible and irrotational:

$$div \ \mathbf{V} = \boldsymbol{\nabla} \cdot \mathbf{V} = \frac{\partial u}{\partial x} + \frac{\partial v}{\partial y} = 0 \quad \text{(Incompressibility)}, \tag{2.2}$$

$$curl \ \mathbf{V} = \boldsymbol{\nabla} \times \mathbf{V} = \left(\frac{\partial v}{\partial x} - \frac{\partial u}{\partial x} \right) \boldsymbol{k} = 0 \quad \text{(Irrotationality)}. \tag{2.3}$$

Due to these equations $\dfrac{d\overline{V}}{d\overline{z}} = 0$ and $\overline{V}(z)$ is complex analytic function.

The fluid particles will follow the trajectories $z(t) = x(t) + iy(t)$, obtained by integrating the differential equations

$$\frac{dx}{dt} = u(x,y), \quad \frac{dy}{dt} = v(x,y). \tag{2.4}$$

In fluid mechanics, the curves parametrized by (2.4) are known as the streamlines, i.e., general definition of a streamline $s(\tau) = z(\tau)$ says that the tangent to the streamline should be equal to the velocity at a given instant in time

$$\frac{dz(\tau)}{d\tau} = V(z), \quad z(0) = z_0, \tag{2.5}$$

where τ is a parameter that characterizes the streamline.

Now, the complex velocity $\overline{V}(z)$ admits a complex anti-derivative, i.e., $\exists$ a complex analytic function

$$\omega(z) = \varphi(x, y) + i\psi(x, y), \tag{2.6}$$

which satisfies $\dfrac{d\omega}{dz} = \overline{V}(z)$. Therefore, we have

$$\frac{\partial \varphi}{\partial x} = u, \qquad \frac{\partial \varphi}{\partial y} = v \tag{2.7}$$

or, $\mathbf{V} = \boldsymbol{\nabla}\varphi$, and hence the real part of the complex function, $\varphi(x, y)$, defines a velocity potential for the fluid flow. For this reason, the anti-derivative $\omega(z)$ is known as a complex potential function for the given fluid velocity field. The harmonic conjugate $\psi(x, y)$ to the velocity potential is known as the stream function. Velocity vector can also be expressed in terms of stream function, i.e., $\mathbf{V} = \boldsymbol{\nabla} \times (\psi \boldsymbol{k})$.

Both the velocity potential and the stream function satisfy the Laplace equation and are related by the Cauchy-Riemann equations

$$\frac{\partial \varphi}{\partial x} = u = \frac{\partial \psi}{\partial y}, \qquad \frac{\partial \varphi}{\partial y} = v = -\frac{\partial \psi}{\partial x}. \tag{2.8}$$

The level sets of the stream function $\{\psi(x, y) = c\}$ where $c \in \mathbb{R}$ are known as the level curves of the stream function, i.e., the streamlines of the flow.

Example 2.1 *Consider the complex potential*

$$\omega = i\kappa \log z, \tag{2.9}$$

where $z = re^{i\theta}$. Then the velocity potential and the stream function are

$$\varphi = -\kappa\theta, \qquad \psi = \kappa \log r. \tag{2.10}$$

The streamlines are concentric circles with center at the origin. This is the fluid flow

induced by a point vortex at the origin.

Next, we give the Milne - Thomson's Circle Theorem (Milne-Thomson 1968) which will be useful when we consider a single cylinder.

2.1. Milne - Thomson's Circle Theorem

Let C be the circle, $|z| = a$, in the z-plane. Let P be the point $z = re^{i\theta}$. Then if Q is the point $\dfrac{a^2}{z}$, we have

$$\frac{a^2}{z} = \frac{a^2}{re^{i\theta}} = \frac{a^2}{r}e^{-i\theta}. \tag{2.11}$$

If we mark, on OP between O and P, the point S such that $|OS| = |OQ| = \dfrac{a^2}{r}$, we see that

$$|OS|.|OP| = a^2. \tag{2.12}$$

Therefore that S and P are inverse points with respect to the circle C and the point Q is the optical reflection of S in the x-axis regarded as a mirror. It is clear from (2.12) that if P is outside the circle ($OP > a$), then S and therefore Q are inside the circle (see Figure 2.1).
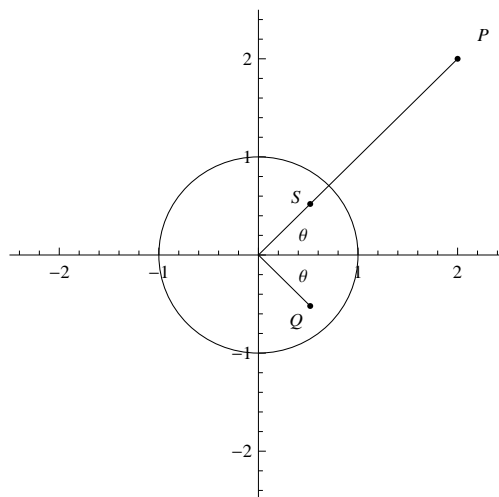
Figure 2.1. S is inverse point of P with respect to C.

If, however, P is on the circumference of the circle, S coincides with P and Q

$$\overline{z} = \frac{a^2}{z}. \tag{2.13}$$

Let $f(z)$ be a function of z which is an analytic in the whole plane except at certain isolated singular points all of which are at a distance greater than a from the origin. We can form the conjugate complex $\overline{f}(\overline{z})$ by replacing i by $-i$ wherever it occurs.

Definition 2.1.0.1 *The function $\overline{f}(z)$ is formed from the function $f(z)$ by first forming $\overline{f}(\overline{z})$ then in $\overline{f}(\overline{z})$ writing z instead of $\overline{z}$.*

We now prove a general theorem which will be of great use.

Theorem 2.1.0.2 *Milne-Thomson Circle Theorem*

Let us consider the irrotational two-dimensional flow of an incompressible inviscid fluid in the z-plane. Let there be no rigid boundaries and let the complex potential of the flow be $f(z)$, where the singularities of $f(z)$ are all at a distance greater than a from the origin. If a circular cylinder, typified by its cross-section of the circle C: $|z| = a$ is introduced into the field of flow, the complex potential becomes

$$\omega = f(z) + \overline{f\left(\frac{a^2}{\overline{z}}\right)} = f(z) + \overline{f}\left(\frac{a^2}{z}\right), \tag{2.14}$$

with (i) the same singularities as $f(z)$ for $|z| > a$ and (ii) $|z| = a$ as a streamline.

Proof 2.1.0.3 *Since $\overline{z} = \dfrac{a^2}{z}$ on the circle, we see that*

$$\omega = f(z) + \overline{f}\left(\frac{a^2}{z}\right) = f(z) + \overline{f}(\overline{z}) \tag{2.15}$$

purely real on the circle C. Thus C is a streamline.

If the point z is outside C, all singularities of $f(z)$ are in the region $|z| > a$, so all the singularities of $\overline{f}\left(\dfrac{a^2}{z}\right)$ are interior to C; in particular $\overline{f}\left(\dfrac{a^2}{z}\right)$ has no singularity at infinity, since $f(z)$ has none at $z = 0$. Thus ω has exactly the same singularities as $f(z)$.

Example 2.2 *Consider a vortex of strength κ at the point z_0 and let the center of the cylinder be at the origin. Here $f(z) = i\kappa \log(z - z_0)$, and therefore, if $|z_0| > a$*

$$\omega = i\kappa \log(z - z_0) - i\kappa \log(\frac{a^2}{z} - \overline{z}_0). \qquad (2.16)$$

Thus $\omega = i\kappa \log(z - z_0) - i\kappa \log(z - \frac{a^2}{\overline{z}_0}) + i\kappa \log(z) + constant$. It is easy to see that on the cylinder ($|z| = a$), the imaginary part of the complex potential (the stream function) vanishes; hence the circle becomes a streamline (see Figures 2.2-2.4).
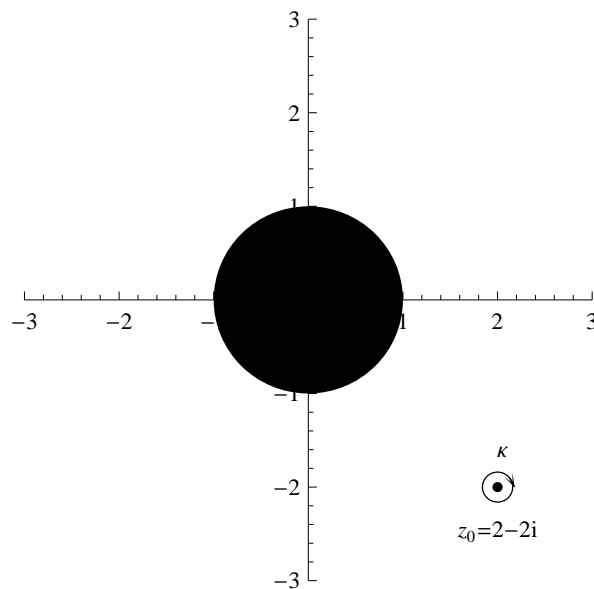
Figure 2.2. Diagram of the physical system represented by vortex-cylinder model, showing one vortex placed at $z_0 = 2 - 2i$ with strength κ and a cylinder with unit radius centred at the origin.

Next we consider the problem of a point vortex and N fixed cylinders in a two - dimensional inviscid fluid and we obtain an analytical−numerical solution in the form of an infinite power series for the velocity field using complex analysis. This problem has been studied in detail by (Pashaev & Yilmaz 2009).

2.2. Two-Dimensional Inviscid Flow around Multiple Cylinders with a Vortex

We formulate the problem of one vortex and N stationary cylinders in an unbounded two-dimensional domain in several steps starting with the case of a single vortex and a single cylinder. For simplicity, we shall take all the circulations around the cylinders to be zero. But in one cylinder and two vortices case we add an independent circulation to the system so that the circulation around the cylinder becomes nonzero.

2.2.1. The Case of a Vortex and a Cylinder

First, consider a vortex of strength κ at z_0 and a cylinder of radius a at the origin. Then the complex potential is given by the Circle Theorem of Milne-Thomson

$$\omega = f(z) + \overline{f}\left(\frac{a^2}{z}\right) = i\kappa \log(z - z_0) - i\kappa \log(\frac{a^2}{z} - \overline{z}_0)$$

$$= i\kappa \log(z - z_0) - i\kappa \log(z - z_0') + i\kappa \log(z) - i\kappa \log(-\overline{z}_0), \qquad (2.17)$$

where $z_0' = \dfrac{a^2}{\overline{z}_0}$ is the inverse point of z_0 with respect to the cylinder. It is easy to see that the imaginary part of the complex potential vanishes on the cylinder hence the boundary condition is satisfied.

Equation (2.17) implies that the effect of the cylinder introduced at the origin is two extra vortices; one of these is at the inverse point of z_0 with negative strength, and another at the center of the cylinder with positive strength. We shall call the vortices at inverse points and at the centres of cylinders (or at infinity) "vortex images". Therefore the effect of the cylinder, introduced at the origin, to the potential is two images, one at the inverse point with negative strength and the other at the centre with positive strength. In Figure 2.3, we see the images of a vortex which is given in Example 2.2.
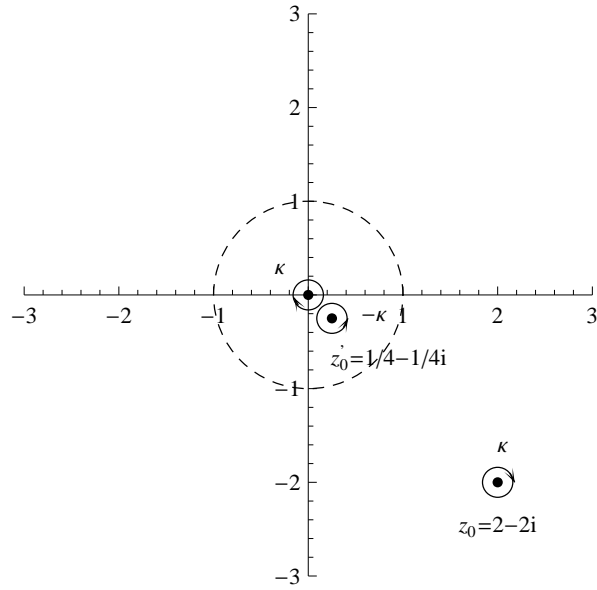
Figure 2.3. Images of one vortex which is considered in example 2.2; one is at the origin with positive strength and the other at the inverse point $z_0' = 1/4 - 1/4i$ with negative strength.

The complex velocity is obtained by differentiating (2.17) with respect to z

$$\overline{V} = \frac{i\kappa}{z - z_0} - \frac{i\kappa}{z - z_0'} + \frac{i\kappa}{z}, \tag{2.18}$$

where $\overline{V} = \dfrac{d\omega}{dz} = u - iv$, with u and v being rectangular components of velocity. Henceforth, we shall work with complex velocity and avoid dealing with the multi-valued function $\log$.

In Figure 2.4, the flow field is shown using equation (2.18) when the vortex is at the point $z_0 = 2 - 2i$ with strength $\kappa = 0.4$ and where the cylinder is at the origin. So this figure represents a vector plot of the velocity field for one vortex outside a cylinder. We see that velocity vectors are tangent to the circle so boundary condition is satisfied, as we expected.
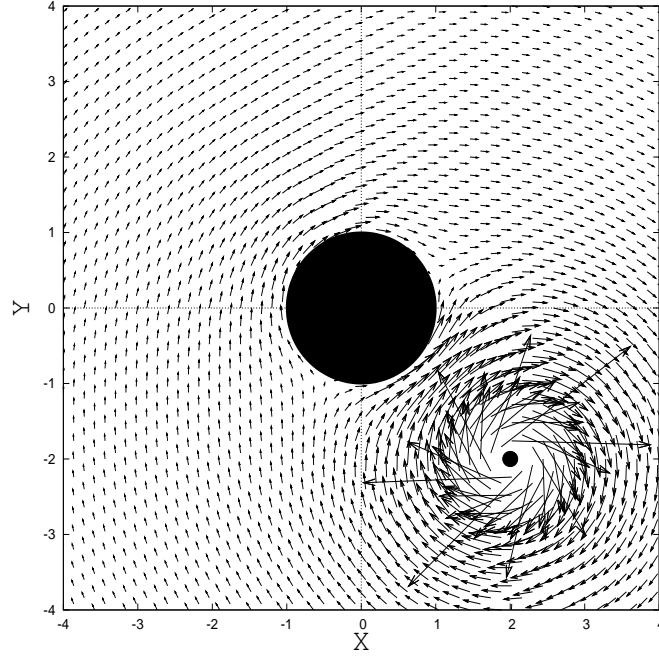
Figure 2.4. Velocity distribution about a cylinder at the origin with a vortex at (2,-2)
with strength 0.4. Velocity vectors are scaled down by a factor of 1.3.

Next we consider a vortex of strength κ at z_0 and a cylinder of radius a_j at z_j. In this case, the complex velocity is obtained by translating the coordinates of the origin to z_j in equation (2.18)

$$
\begin{aligned}
\overline{V} &= \frac{i\kappa}{z - z_0} - \frac{i\kappa}{z - z_j - (z_0 - z_j)'} + \frac{i\kappa}{z - z_j} \\
&= \frac{i\kappa}{\zeta_j - \zeta_{0j}} - \frac{i\kappa}{\zeta_j - \zeta'_{0j}} + \frac{i\kappa}{\zeta_j} = \overline{V}_j^I + \overline{V}_j^D,
\end{aligned}
\tag{2.19}
$$

where $\zeta_j = z - z_j$, $\zeta_{0j} = z_0 - z_j$ and $\zeta'_{0j} = a_j^2/\overline{\zeta}_{0j}$. The term

$$
\overline{V}_j^I = \frac{i\kappa}{\zeta_j - \zeta_{0j}},
\tag{2.20}
$$

in equation (2.19) represents the velocity field due to the vortex alone and the term

$$\overline{V}_j^D = \frac{i\kappa}{\zeta_j} - \frac{i\kappa}{\zeta_j - \zeta_{0j}'} \qquad (2.21)$$

represents the effect of the cylinder on the velocity field.

For the general problem of arbitrary number of cylinders and vortices, we shall need the Laurent series of the terms in (2.19) around z_j. We start with the first term

$$\overline{V}_j^I = \frac{i\kappa}{\zeta_j - \zeta_{0j}} = -\frac{i\kappa}{\zeta_{0j}} \sum_{n=0}^{\infty} \left(\frac{\zeta_j}{\zeta_{0j}}\right)^n \ , \ |\zeta_j| < |\zeta_{0j}|. \qquad (2.22)$$

Here we assume that the centre of the vortex is outside the cylinder. In this case the condition $|\zeta_j| < |\zeta_{0j}|$ is certainly true when the boundary condition is applied on the cylinder ($z = z_j + a_j e^{i\theta_j}$).

The last two terms in equation (2.19) are treated together

$$\overline{V}_j^D = \frac{i\kappa}{\zeta_j} - \frac{i\kappa}{\zeta_j - \zeta_{0j}'} = -i\kappa \sum_{n=1}^{\infty} \frac{(\zeta_{0j}')^n}{\zeta_j^{n+1}}, \qquad (2.23)$$

where $\zeta_{0j}' = a_j^2/\overline{\zeta}_{0j}$ implies $|\zeta_{0j}'| \le |\zeta_j|$, and corresponds to the vortex images.

In Figure 2.5 the flow field is shown when the vortex is at the point $z_0 = 2 + 2i$ with strength $\kappa = -0.4$ and the cylinder is at the point $z_j = -1 - i$.

2.2.2. Force on the Cylinder

First we will state the Blasius' Theorem which is used to calculate the force on the cylinders without proof. Let a fixed cylinder be placed in an incompressible and irrotational flow field. If ω is the complex potential then the theorem of Blasius is as follows

$$\overline{F} = \frac{i\rho}{2} \oint_C \left(\frac{d\omega}{dz}\right)^2 dz, \qquad (2.24)$$
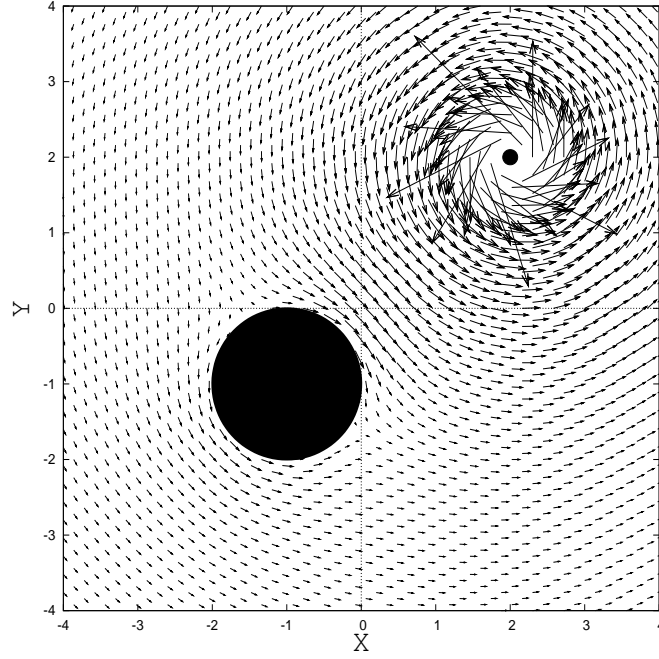
Figure 2.5. Velocity distribution about a cylinder at the point $(-1, -1)$ with a vortex at (2,2) with strength -0.4. Velocity vectors are scaled down by the factor of 1.3.

where ρ is the mass density of the fluid and $\overline{F}$ denotes complex conjugate of the force $F = F_x + iF_y$ on the system and the integral is taken around the cylinder. We can rewrite equation (2.24) using

$$\left(\frac{d\omega}{dz}\right)^2 = \overline{V}^2. \tag{2.25}$$

Therefore, we need the square of the velocity for this purpose, namely,

$$\overline{V}^2 = -\kappa^2 \left(\frac{1}{(\zeta_j - \zeta_{0j})^2} + \frac{1}{(\zeta_j - \zeta'_{0j})^2} + \frac{1}{\zeta_j^2} + \right.$$

$$\left. + \frac{2}{\zeta_j(\zeta_j - \zeta_{0j})} - \frac{2}{(\zeta_j - \zeta_{0j})(\zeta_j - \zeta'_{0j})} - \frac{2}{\zeta_j(\zeta_j - \zeta'_{0j})} \right) \tag{2.26}$$

13

If we integrate equation (2.26) with respect to ζ_j around the cylinder we have

$$
\begin{aligned}
\overline{F} &= \frac{i\rho}{2} \int\limits_{|\zeta_j|=a_j} \overline{V}^2 d\zeta_j = 2\pi\rho\kappa^2 \left(\frac{1}{\zeta_{0j} - \zeta'_{0j}} - \frac{1}{\zeta_{0j}} \right) \\
&= 2\pi\rho a_j^2 \kappa^2 \left(\frac{\overline{z_0} - \overline{z_j}}{|z_0 - z_j|^2 \left(|z_0 - z_j|^2 - a_j^2 \right)} \right).
\end{aligned}
\tag{2.27}
$$

If we write $z_0 = x_0 + iy_0$ and $z_j = x_j + iy_j$ in equation (2.27) we have

$$
F_x = 2\pi\rho a_j^2 \kappa^2 \left(\frac{x_0 - x_j}{|z_0 - z_j|^2 \left(|z_0 - z_j|^2 - a_j^2 \right)} \right)
\tag{2.28}
$$

$$
F_y = -2\pi\rho a_j^2 \kappa^2 \left(\frac{y_0 - y_j}{|z_0 - z_j|^2 \left(|z_0 - z_j|^2 - a_j^2 \right)} \right).
\tag{2.29}
$$

Now we calculate the circulation around the cylinder which is the line integral of the tangential component of the velocity taken around the circle, given by

$$
\Gamma = \oint_C V_t ds = \oint_C u dx + v dy = Re \left(\oint_C \overline{V} dz \right),
\tag{2.30}
$$

where C denotes the circle and $V_t = Re(\overline{V} i e^{i\theta})$ is the tangential component of $\overline{V}$. Using Cauchy's Theorem we get

$$
\begin{aligned}
\Gamma &= Re \left(\int\limits_{|\zeta_j|=a_j} \overline{V} i a e^{i\theta} d\theta \right) = Re \left(\int\limits_{|\zeta_j|=a_j} i\kappa \left(\frac{1}{\zeta_j - \zeta_{0j}} - \frac{1}{\zeta_j - \zeta'_{0j}} + \frac{1}{\zeta_j} \right) d\zeta_j \right) \\
&= Re \left(i\kappa \left(-2\pi i + 2\pi i \right) \right) = 0.
\end{aligned}
\tag{2.31}
$$

This is expected since the strengths of image at the centre and at the inverse point are of equal in magnitude and opposite in sign. Therefore, their total effect on the boundary is zero when evaluating equation (2.30).

2.2.3. The Case of a Vortex and N-Cylinders

Now we assume that there are N cylinders of radii $a_1, ...a_N$ placed in an unbounded two-dimensional fluid domain at points $z_1, ..., z_N$ and that a vortex is placed at z_0 outside the cylinders (Pashaev & Yilmaz 2009). In order to apply the boundary conditions at the boundaries of the cylinders, we express the total velocity near cylinder j by

$$\overline{V}_j^T \;=\; \overline{V}_j^I + \overline{V}_j^D + \sum_{\substack{i=1 \\ i \neq j}}^{N} \overline{V}_i^D, \tag{2.32}$$

where

$$\overline{V}_j^I \;=\; -\frac{i\kappa}{\zeta_{0j}} \sum_{n=0}^{\infty} \left(\frac{\zeta_j}{\zeta_{0j}} \right)^n \;,\;\; |\zeta_j| < |\zeta_{0j}|, \tag{2.33}$$

$$\overline{V}_j^D \;=\; -i\kappa \sum_{n=1}^{\infty} A_n^j \frac{(\zeta_{0j}')^n}{\zeta_j^{n+1}} \;,\;\; |\zeta_{0j}'| \leq |\zeta_j|, \tag{2.34}$$

$$\overline{V}_i^D \;=\; -i\kappa \sum_{n=1}^{\infty} A_n^i \frac{(\zeta_{0i}')^n}{\zeta_i^{n+1}} = -i\kappa \sum_{n=1}^{\infty} A_n^i \frac{(\zeta_{0i}')^n}{(\zeta_j + R_{ij})^{n+1}} \tag{2.35}$$

and A_n^i are unknown complex coefficients. We see that for the case of a single cylinder the unknown coefficients A_n^j in equation (2.34) become unity. The first term in (2.32) represents the velocity field due to the vortex, whereas the second and third terms account for the effects of the cylinders and they describe a set of images in cylinders and the images of images.

The boundary condition to be satisfied for each cylinder is that "the normal component of $\overline{V}_j^T = 0$, when $|\zeta_j| = a_j, \forall j$". This condition is equivalent to the statement

$$a_j Re(\overline{V}_j^T e^{i\theta_j}) = Re(\overline{V}_j^T a_j e^{i\theta_j}) = Re(\overline{V}_j^T \zeta_j) = 0, \;\; j = 1, ..., N \tag{2.36}$$

where $Re(z)$ denotes the real part of z. In the last equality $\zeta_j = a_j e^{i\theta_j}$ is used, this holds

only on the boundary of cylinder j. Application of this condition yields

$$Re\left(-i\kappa\left(\sum_{n=0}^{\infty}\frac{\zeta_j^{n+1}}{\zeta_{0j}^{n+1}}+\sum_{n=1}^{\infty}\frac{B_n^j}{\zeta_j^n}+\sum_{i=1}^{N}(1-\delta_{ij})\sum_{n=1}^{\infty}\frac{B_n^i\zeta_j}{(\zeta_j+R_{ij})^{n+1}}\right)\right)=0, \quad (2.37)$$

where $B_n^j=A_n^j\dfrac{a_j^{2n}}{\zeta_{0j}^n}$ and $\delta_{ij}=1$ when $i=j$, $\delta_{ij}=0$ otherwise. The last term in (2.37) must be expanded into a series

$$\frac{1}{(\zeta_j+R_{ij})^{n+1}}=\frac{1}{R_{ij}^{n+1}}\sum_{k=0}^{\infty}\frac{(n+1)_k}{k!}\left(-\frac{\zeta_j}{R_{ij}}\right)^k, \quad (2.38)$$

where $(n+1)_k=(n+1)(n+2)...(n+k)$ is the Pochhammer symbol and $(n+1)_0=1$. Then the algebraic system for the unknown coefficients B_l^s is

$$\sum_{l=1}^{\infty}\sum_{s=1}^{N}D_{nl}^{js}B_l^s=C_n^j, \quad j=1,...,N, \quad n=0,1,... \quad (2.39)$$

where

$$\begin{aligned}D_{nl}^{js} &= -\frac{\delta_{n+1,l}\delta_{j,s}}{a_j^{2n+2}}+\frac{(-1)^n}{n!}\sum_{k=1}^{\infty}\sum_{i=1}^{N}(1-\delta_{si})(1-\delta_{ij}) \\ &\quad \times\frac{(-1)^{k-1}}{(k-1)!}\frac{a_i^{2k}(k+1)_n(l+1)_{k-1}}{R_{si}^{k+l}\overline{R}_{ij}^{n+k+1}},\end{aligned} \quad (2.40)$$

$$C_n^j = \frac{-1}{\overline{\zeta}_{0j}^{n+1}}-\frac{(-1)^n}{n!}\sum_{i=1}^{N}(1-\delta_{ij})\sum_{k=1}^{\infty}\frac{(k+1)_na_i^{2k}}{\overline{R}_{ij}^{n+k+1}}\frac{1}{\zeta_{0i}^k}. \quad (2.41)$$

We notice that with a single cylinder, the above system gives $B_n^j=\dfrac{a_j^{2n}}{\zeta_{0j}^n}$, which is equivalent to $A_n=1$ as expected.

In Figure 2.6 flow field is shown when the vortex is at the point $z_0 = 1.6i$ with strength $\kappa = 0.4$ and two cylinders of unit radii, one placed at the origin and another at the point $(3, 0)$.
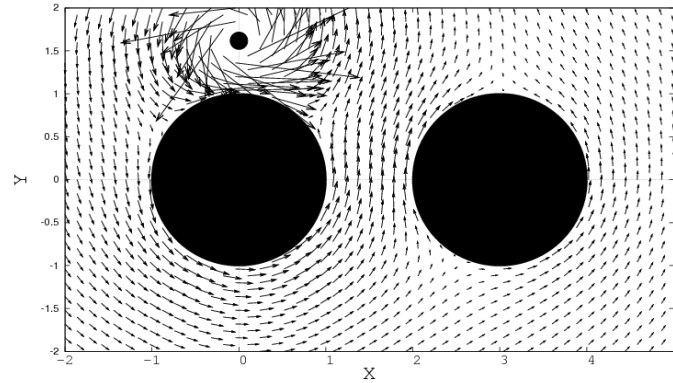
Figure 2.6. Velocity distribution about two cylinders at the points $(0, 0)$ and $(3, 0)$ with a vortex at (0,1.6) with strength -0.4. Velocity vectors are scaled down by the factor of 1.3.

In Figure 2.7 we consider an example of four disks placed at the corners of a square, $\zeta_1 = 2 + 2i$, $\zeta_2 = -2 + 2i$, $\zeta_2 = -2 - 2i$ and $\zeta_4 = 2 - 2i$, when the vortex is at the point $z_0 = 0$ with strength $\kappa = 0.4$ and the cylinders at the points. This resembles the legs of a Tension Leg Platform (TLP).
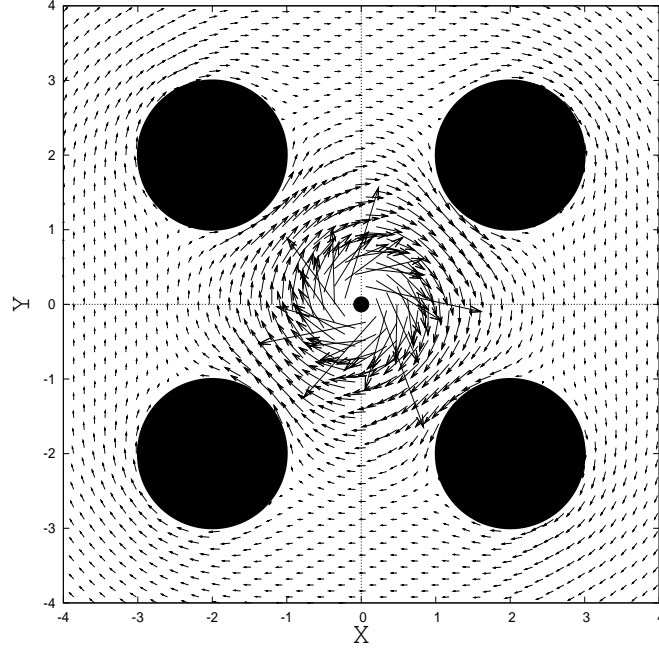
Figure 2.7. Velocity distribution about four cylinders at the points $(2, 2)$, $(-2, 2)$, $(-2, -2)$ and $(-2, 2)$ with a vortex at (0,0) with strength -0.4. Velocity vectors are scaled down by the factor of 1.3.

We need again the square of $\overline{V}_j^T$ to calculate the force on the system

$$
\begin{aligned}
\left(\overline{V}_j^T\right)^2 &= \left(\overline{V}_j^I + \overline{V}_j^D + \sum_{\substack{i=1 \\ i \neq j}}^{N} \overline{V}_i^D\right)^2 \\
&= \left(\overline{V}_j^I\right)^2 + \left(\overline{V}_j^D\right)^2 + \sum_{\substack{i=1 \\ i \neq j}}^{N} \sum_{\substack{k=1 \\ k \neq j}}^{N} \overline{V}_i^D \overline{V}_k^D \\
&\quad + 2\overline{V}_j^I \overline{V}_j^D + 2\overline{V}_j^I \sum_{\substack{i=1 \\ i \neq j}}^{N} \overline{V}_i^D + 2\overline{V}_j^D \sum_{\substack{i=1 \\ i \neq j}}^{N} \overline{V}_i^D,
\end{aligned} \tag{2.42}
$$

where,

$$\left(\overline{V}_j^I\right)^2 = \frac{-\kappa^2}{\zeta_{0j}^2} \sum_{n=0}^{\infty} \sum_{m=0}^{\infty} \left(\frac{\zeta_j}{\zeta_{0j}}\right)^{n+m}, \tag{2.43}$$

$$\left(\overline{V}_j^D\right)^2 = -\kappa^2 \sum_{n=1}^{\infty} \sum_{m=1}^{\infty} A_n^j A_m^j \frac{(\zeta_{0j}')^{n+m}}{\zeta_j^{n+m+2}}, \tag{2.44}$$

$$\overline{V}_i^D \overline{V}_k^D = \sum_{n=1}^{\infty} \sum_{m=1}^{\infty} A_n^j A_m^j \frac{(\zeta_{0i}')^n (\zeta_{0j}')^m}{(\zeta_j + R_{ij})^{n+1}(\zeta_j + R_{kj})^{m+1}}, \tag{2.45}$$

$$\overline{V}_j^I \overline{V}_j^D = \frac{-\kappa^2}{\zeta_{0j}} \sum_{n=0}^{\infty} \sum_{m=1}^{\infty} A_m^j \frac{\zeta_j^n (\zeta_{0j}')^m}{\zeta_{0j}^n \zeta_j^{m+1}}, \tag{2.46}$$

$$\overline{V}_j^I \sum_{\substack{i=1 \\ i \neq j}}^{N} \overline{V}_i^D = \frac{-\kappa^2}{\zeta_{0j}} \sum_{n=0}^{\infty} \sum_{m=1}^{\infty} A_m^i \frac{\zeta_j^n (\zeta_{0i}')^m}{\zeta_{0j}^n (\zeta_j + R_{ij})^{m+1}}, \tag{2.47}$$

$$\overline{V}_j^D \sum_{\substack{i=1 \\ i \neq j}}^{N} \overline{V}_i^D = -\kappa^2 \sum_{n=1}^{\infty} \sum_{m=1}^{\infty} A_n^j A_m^i \frac{(\zeta_{0j}')^n (\zeta_{0i}')^m}{\zeta_j^{n+1}(\zeta_j + R_{ij})^{m+1}}. \tag{2.48}$$

If we integrate equation (2.42) with respect to ζ_j around cylinder j, we see that the terms (2.43), (2.44), (2.45) and (2.47) give a zero contribution. Then by Blasius' Theorem, the force on the system is given by

$$\overline{F} = \frac{i\rho}{2} \int_{|\zeta_j|=a_j} \left(\overline{V}_j^T\right)^2 d\zeta_j = \frac{2\pi\rho\kappa^2}{\zeta_{0j}} \sum_{n=1}^{\infty} \frac{(\zeta_{0j}')^n}{\zeta_{0j}^n} A_n^j$$

$$+ 2\pi\rho\kappa^2 \sum_{n=1}^{\infty} \sum_{m=1}^{\infty} (-1)^n A_n^j A_m^i \frac{(\zeta_{0j}')^n (\zeta_{0i}')^m}{(R_{ij})^{m+n+1}} \frac{(n+1)_n}{n!}. \tag{2.49}$$

We can check that $\overline{F}$ reduces to the one cylinder case. If we have one cylinder, all coefficients A_n^j become unity and the term $\overline{V}_i^D$ become zero. Since $|\zeta_{0j}'| < |\zeta_{0j}|$, $\overline{F}$ becomes

$$\overline{F} = \frac{2\pi\rho\kappa^2}{\zeta_{0j}} \sum_{n=1}^{\infty} \frac{(\zeta_{0j}')^n}{\zeta_{0j}^n} = \frac{2\pi\rho\kappa^2}{\zeta_{0j}} \left(\frac{\zeta_{0j}}{\zeta_{0j} - \zeta_{0j}'} - 1\right)$$

$$= 2\pi\rho\kappa^2 \left(\frac{1}{\zeta_{0j} - \zeta_{0j}'} - \frac{1}{\zeta_{0j}}\right), \tag{2.50}$$

which is the same result as in equation (2.27).

And using Cauchy's Theorem we can calculate the circulation around the j-th cylinder

$$
\Gamma = Re\left(\oint_{|\zeta_j|=a_j} \overline{V}_j^T d\zeta_j\right) = Re\left(\oint_{|\zeta_j|=a_j} \left(\overline{V}_j^I + \overline{V}_j^D + \sum_{\substack{i=1 \\ i\neq j}}^{N} \overline{V}_i^D\right) d\zeta_j\right) = 0,
$$

as we expected.

2.3. Flow around a Cylinder and Two Vortices

Now we assume that a cylinder is placed at z_j of radius a in an unbounded two-dimensional fluid domain and two vortices with strengths κ_1, κ_2 are placed at z_{01}, z_{02} outside the cylinder (Tülü & Yilmaz 2010). The complex potential is given by the Circle Theorem,

$$
\begin{aligned}
\omega &= f(\zeta_j) + \overline{f}\left(\frac{a^2}{\zeta_j}\right) \\[2mm]
&= i\kappa_1 \log(\zeta_j - \zeta_{1j}) + i\kappa_2 \log(\zeta_j - \zeta_{2j}) \\[2mm]
&\quad - i\kappa_1 \log\left(\frac{a^2}{\zeta_j} - \overline{\zeta}_{1j}\right) - i\kappa_2 \log\left(\frac{a^2}{\zeta_j} - \overline{\zeta}_{2j}\right),
\end{aligned}
\tag{2.51}
$$

where $\zeta_j = z - z_j$, $\zeta_{1j} = z_{01} - z_j$, $\zeta_{2j} = z_{02} - z_j$.

The first two terms in (2.51) are complex potentials of the two vortices and the last two terms represent the effect of the cylinder. It is easy to see that on the cylinder, that is when $\zeta_j\overline{\zeta}_j = a^2$, the imaginary part of the complex potential, the stream function, vanishes hence the boundary condition is satisfied

$$
\omega = \varphi + i\psi = f(\zeta_j) + \overline{f}(\overline{\zeta}_j) \in \mathbb{R}.
\tag{2.52}
$$

After some simple manipulations we can rewrite the complex potential as

$$\omega = i\kappa_1 \log(\zeta_j - \zeta_{1j}) - i\kappa_1 \log(\zeta_j - \zeta'_{1j}) + i\kappa_1 \log(\zeta_j) - i\kappa_1 \log(-\overline{\zeta}_{1j})$$

$$+i\kappa_2 \log(\zeta_j - \zeta_{2j}) - i\kappa_1 \log(\zeta_j - \zeta'_{2j}) + i\kappa_2 \log(\zeta_j) - i\kappa_2 \log(-\overline{\zeta}_{2j}), \quad (2.53)$$

where $\zeta'_{1j} = \dfrac{a^2}{\overline{\zeta}_{1j}}$ and $\zeta'_{2j} = \dfrac{a^2}{\overline{\zeta}_{2j}}$. We notice that in equation (2.53) there are two images for each vortex; one at the symmetric point of the vortex with respect to the cylinder, another one at the center of the cylinder. While the first image has the negative strength, the latter has the positive strength.

We should remark that the image vortex at the center of the cylinder is not necessary to satisfy the boundary condition, for a vortex at the center of the cylinder will give only tangential component on the boundary of the cylinder. The effect of the image at the center which has the same strength but opposite sign to the one at the symmetric point is to produce zero circulation on the circle. It is possible to generalize the problem by making the strength of the image at the center different from the one at the inverse point and therefore to have nonzero circulation around the cylinder. However, as we shall see, zero circulation does not necessarily mean zero force.

The complex velocity is obtained by differentiating the equation (2.53)

$$\overline{V} = \frac{i\kappa_1}{\zeta_j - \zeta_{1j}} - \frac{i\kappa_1}{\zeta_j - \zeta'_{1j}} + \frac{i\kappa_1}{\zeta_j}$$

$$+\frac{i\kappa_2}{\zeta_j - \zeta_{2j}} - \frac{i\kappa_2}{\zeta_j - \zeta'_{2j}} + \frac{i\kappa_2}{\zeta_j}, \quad (2.54)$$

where $\overline{V} = \dfrac{d\omega}{dz} = u - iv$.

In Figure 2.8 flow field is shown when the two vortices have the same strength. We see that at the bisector of the line joining the centers of two vortices, there is a stagnation point which means the velocity is zero at this point. Whereas in Figure 2.9 where total strength of vortices vanishes there are no stagnation points. Also the force acting on the cylinder is 80 times higher in the latter case.
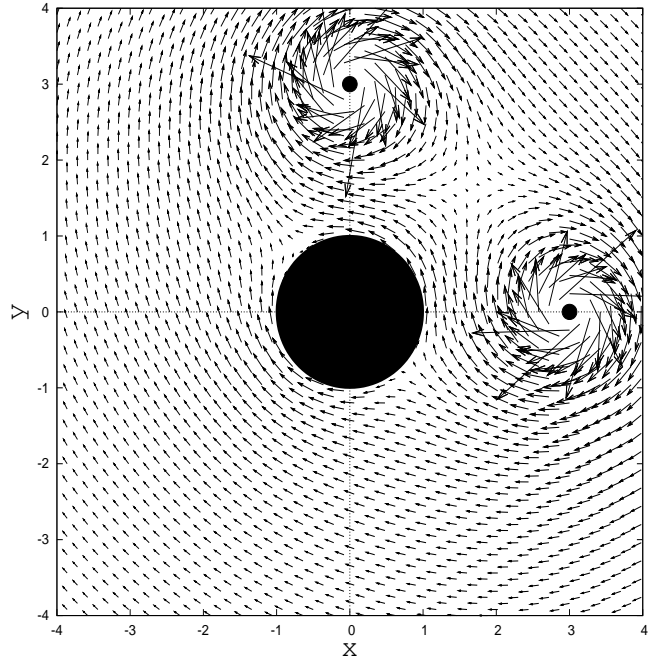
Figure 2.8. Velocity distribution about a cylinder at the origin with two vortices of unit strength. Velocity vectors are scaled down by the factor of 1.3.
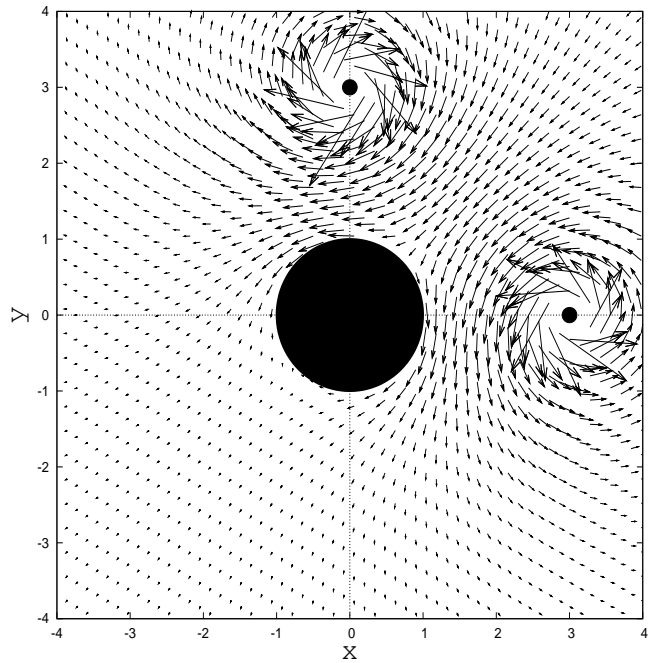
Figure 2.9. Velocity distribution about a cylinder at the origin with two vortices of vanishing total strength. Velocity vectors are scaled down by the factor of 1.3.

Before we calculate the force on the cylinder, we shall generalize equation (2.54) by making the strength at the center of the cylinder arbitrary

$$
\begin{aligned}
\overline{V} &= \frac{i\kappa_1}{\zeta_j - \zeta_{1j}} - \frac{i\kappa_1}{\zeta_j - \zeta'_{1j}} + \frac{i\kappa_0}{\zeta_j} \\
&+ \frac{i\kappa_2}{\zeta_j - \zeta_{2j}} - \frac{i\kappa_2}{\zeta_j - \zeta'_{2j}}.
\end{aligned} \tag{2.55}
$$

By Blasius' Theorem, the force on the system is given by

$$
\begin{aligned}
\overline{F} = \frac{i\rho}{2} \int\limits_{|\zeta_j|=a} \overline{V}^2 dz &= 2\pi\rho\kappa_1^2 \left(\frac{1}{\zeta_{1j} - \zeta'_{1j}} \right) + 2\pi\rho\kappa_2^2 \left(\frac{1}{\zeta_{2j} - \zeta'_{2j}} \right) \\
&+ 2\pi\rho\kappa_1\kappa_2 \left(\frac{1}{\zeta_{1j} - \zeta'_{2j}} + \frac{1}{\zeta_{2j} - \zeta'_{1j}} \right) - 2\pi\rho\kappa_0 \left(\frac{\kappa_1}{\zeta_{1j}} + \frac{\kappa_2}{\zeta_{2j}} \right).
\end{aligned} \tag{2.56}
$$

Notice that the circulation around the cylinder depends on the value of κ_0

$$
\begin{aligned}
\Gamma &= Re \left(\int\limits_{|\zeta_j|=a} i\kappa_1 \left(\frac{1}{\zeta_j - \zeta_{1j}} - \frac{1}{\zeta_j - \zeta'_{1j}} \right) dz \right) \\
&+ Re \left(\int\limits_{|\zeta_j|=a} i\kappa_2 \left(\frac{1}{\zeta_j - \zeta_{2j}} - \frac{1}{\zeta_j - \zeta'_{2j}} \right) dz \right) \\
&+ Re \left(\int\limits_{|\zeta_j|=a} i\kappa_0 \left(\frac{1}{\zeta_j} \right) dz \right) \\
&= 2\pi(\kappa_1 + \kappa_2 - \kappa_0),
\end{aligned} \tag{2.57}
$$

when $\kappa_0 = \kappa_1 + \kappa_2$, circulation would be zero, as expected.

A simple analysis of equation (2.56) shows that force on the cylinder becomes zero under certain conditions; when vortices have the same strength ($\kappa_1 = \kappa_2$), are equidistant from the centre of the cylinder and are placed symmetrically with respect to the centre. Maximum force would occur in the limiting case when the same-sign vortices collide.

Instead of $\kappa_1 = \kappa_2$, if we assume that $\kappa_1 = -\kappa_2$ then κ_0 must be zero for force to be zero under the same conditions as before.

2.4. The Vortex Doublet

First we consider the case of only two vortices placed at the points z_{01} and z_{02} satisfying $|z_{01} - z_{02}| < \epsilon$ with opposite circulation $\kappa_1 = -\kappa_2 = \kappa$ in an unbounded two-dimensional fluid domain. The complex velocity is given by

$$\overline{V} = i\kappa \left(\frac{1}{z - z_{01}} - \frac{1}{z - z_{02}} \right) = \frac{i\kappa\epsilon e^{i\theta}}{(z - z_{01})(z - z_{02})}, \qquad (2.58)$$

where θ is the angle between the line joining vortices and $x-$axis. Notice that when ϵ approaches to zero vortices are merging. So if we let $\epsilon \to 0$ and choose $\kappa = \dfrac{k}{\epsilon}$ then we get a vortex doublet with strength k, and complex velocity becomes

$$\overline{V} = \frac{ike^{i\theta}}{(z - z_{01})^2}. \qquad (2.59)$$
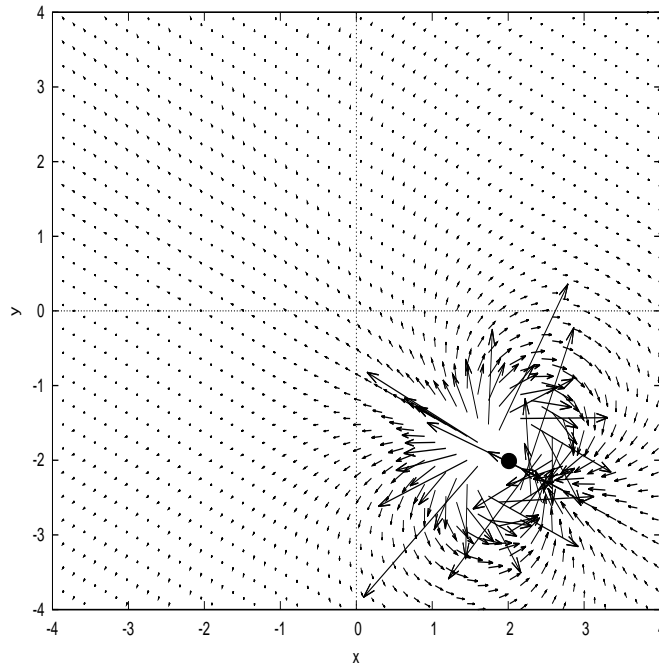
Figure 2.10. Velocity distribution of a vortex doublet where $\theta = \frac{\pi}{3}$ and $k = 0.4$. Velocity vectors are scaled down by the factor of 1.3.

In Figure 2.10 velocity distribution of a vortex doublet is shown using equation (2.59). Here we choose the angle $\theta = \dfrac{\pi}{3}$ and the strength $k = 0.4$. If we integrate equation (2.59) with respect to z we can find complex potential of the system

$$\omega = -\frac{ike^{i\theta}}{(z - z_{01})}. \tag{2.60}$$

Now we insert a cylinder to the system with radius a and centred at the origin. Since we have a single cylinder we can use Milne-Thomson's Circle Theorem to derive the complex potential

$$\omega = -\frac{ike^{i\theta}}{(z - z_{01})} + \frac{ike^{-i\theta}}{\left(\dfrac{a^2}{z} - \bar{z}_{01}\right)}. \tag{2.61}$$

We differentiate equation (2.61) with respect to z to derive the complex velocity

$$\overline{V} = \frac{ike^{i\theta}}{(z - z_{01})^2} + \frac{ika^2 e^{-i\theta}}{z^2 \left(\dfrac{a^2}{z} - \bar{z}_{01}\right)^2}. \tag{2.62}$$

Thus we define a vortex doublet about a cylinder with radius a and centred at the origin. In Figure 2.11 velocity distribution of a vortex doublet about a single cylinder is shown using equation (2.62).

The pairing process of vortices is one of the main building blocks of fluid motion and plays a major role in a variety of fluid phenomena. Its potential significance covers various fields such as geophysics, meteorology, and astrophysics. The merger of two vortices in a two-dimensional incompressible fluid has been studied by many authors. In (Maze, Carton & Lapeyre 2004), (Meunier, Ehrenstein, Leweke & Rossi 2002) a critical distance which vortices do not merge, has been found for a pair of equal two-dimensional vortices. In (Maze, Carton & Lapeyre 2004) equal and positive vorticity was chosen for the vortices and in (Meunier, Ehrenstein, Leweke & Rossi 2002) co-rotating vortices are considered.
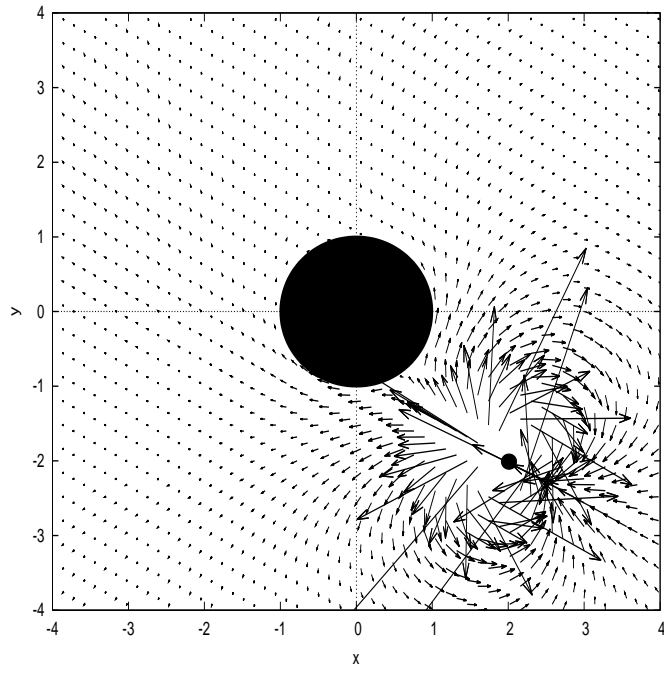
Figure 2.11. Velocity distribution of a vortex doublet where $\theta = \frac{\pi}{3}$ and $k = 0.4$. Velocity vectors are scaled down by the factor of 1.3.

2.5. Uniform Flow around a Cylinder and Two Vortices

Now we formulate the problem of two vortices, a uniform flow and a stationary cylinders in unbounded two dimensional domain. We assume that a cylinder of radius a is placed at z_j in an unbounded two-dimensional fluid domain where two point vortices with strengths κ_1, κ_2 are located outside the cylinder at points z_{01}, z_{02} respectively. There is a uniform flow with velocity $-iu_0$ at infinity. (See Figure 2.12.)
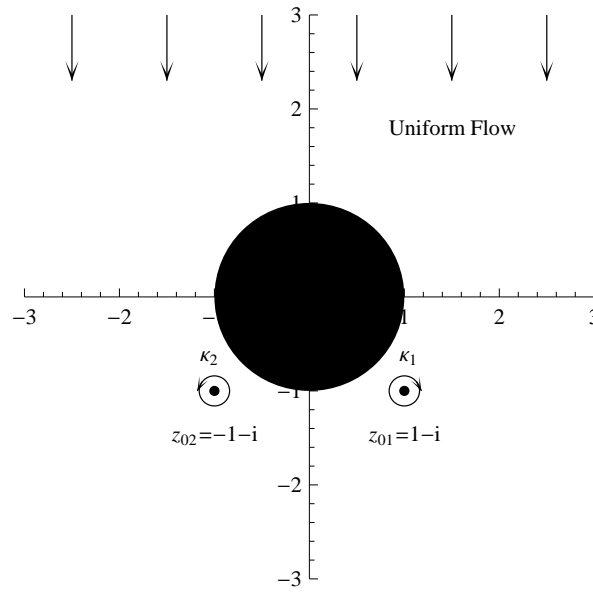
Figure 2.12. Diagram of the physical system represented by vortices-cylinder model, showing uniform flow field, two vortices placed at $z_{01} = 1 - i$ and $z_{02} = -1-i$ with opposite strengths κ_1, κ_2 and a cylinder with unit radius centred at the origin.

The complex potential is given by the Circle Theorem

$$
\begin{aligned}
\omega \;=\; & iu_0\zeta_j + i\kappa_1 \log(\zeta_j - \zeta_{1j}) + i\kappa_2 \log(\zeta_j - \zeta_{2j}) \\[2mm]
& -iu_0\frac{a^2}{\zeta_j} - i\kappa_1 \log\left(\frac{a^2}{\zeta_j} - \overline{\zeta}_{1j}\right) - i\kappa_2 \log\left(\frac{a^2}{\zeta_j} - \overline{\zeta}_{2j}\right),
\end{aligned}
\qquad (2.63)
$$

where $\zeta_j = z - z_j$, $\zeta_{1j} = z_{01} - z_j$, $\zeta_{2j} = z_{02} - z_j$ and u_0 is the constant fluid velocity at infinity. The first three terms in (2.63) are complex potentials of the two vortices and the uniform flow and the last three terms represent the effect of the cylinder. It easy to see

27

that when $\zeta_j \overline{\zeta}_j = a^2$ complex potential becomes

$$\omega = \varphi + i\psi = f(\zeta_j) + \overline{f}(\overline{\zeta}_j) \in \mathbb{R}, \tag{2.64}$$

hence the boundary condition is satisfied. We can rewrite the complex potential as

$$\begin{aligned}
\omega = {} & iu_0 \left(\zeta_j - \frac{a^2}{\zeta_j} \right) + i\kappa_1 \log(\zeta_j - \zeta_{1j}) - i\kappa_1 \log(\zeta_j - \zeta'_{1j}) \\[2ex]
& + i\kappa_1 \log(\zeta_j) - i\kappa_1 \log(-\overline{\zeta}_{1j}) + i\kappa_2 \log(\zeta_j - \zeta_{2j}) \\[2ex]
& - i\kappa_1 \log(\zeta_j - \zeta'_{2j}) + i\kappa_2 \log(\zeta_j) - i\kappa_2 \log(-\overline{\zeta}_{2j}),
\end{aligned} \tag{2.65}$$

where $\zeta'_{1j} = \dfrac{a^2}{\overline{\zeta}_{1j}}$ and $\zeta'_{2j} = \dfrac{a^2}{\overline{\zeta}_{2j}}$. The complex velocity is obtained by differentiating equation (2.65)

$$\begin{aligned}
\overline{V} = {} & iu_0 \left(1 + \frac{a^2}{\zeta_j^2} \right) + \frac{i\kappa_1}{\zeta_j - \zeta_{1j}} - \frac{i\kappa_1}{\zeta_j - \zeta'_{1j}} + \\[2ex]
& + \frac{i\kappa_1}{\zeta_j} + \frac{i\kappa_2}{\zeta_j - \zeta_{2j}} - \frac{i\kappa_2}{\zeta_j - \zeta'_{2j}} + \frac{i\kappa_2}{\zeta_j},
\end{aligned} \tag{2.66}$$

where $\overline{V} = \dfrac{d\omega}{dz} = u - iv$.

Figure 2.13 shows the velocity distribution around a cylinder in uniform flow with two vortices of opposing strengths. We see that there is a stagnation point on y axis just below the cylinder at $y = -1.815$.

Again we will generalize equation (2.66) by making the strength at the center of the cylinder arbitrary

$$\begin{aligned}
\overline{V} = {} & iu_0 \left(1 + \frac{a^2}{z^2} \right) + \frac{i\kappa_1}{z - z_{01}} - \frac{i\kappa_1}{z - z'_1} + \frac{i\kappa_0}{z} \\[2ex]
& + \frac{i\kappa_2}{z - z_{02}} - \frac{i\kappa_2}{z - z'_2}.
\end{aligned} \tag{2.67}$$
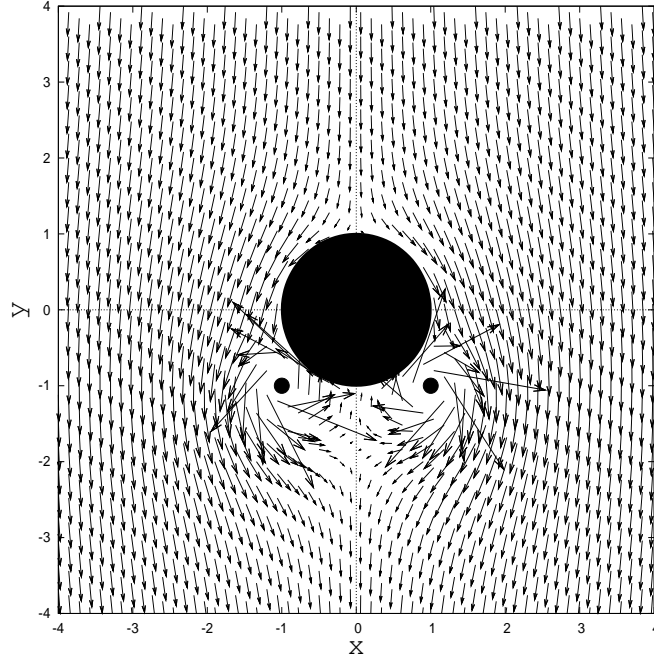
Figure 2.13. Velocity distribution about a cylinder at the origin with two vortices of vanishing total strength in the presence of uniform velocity. $u_0 = 1$.

By Blasius' Theorem, the force on the system is given by

$$\overline{F} = \frac{i\rho}{2} \int\limits_{|z|=a} \overline{V}^2 dz = 2\pi\rho\kappa_1^2 \left(\frac{1}{\zeta_{1j} - \zeta'_{1j}} \right) + 2\pi\rho\kappa_2^2 \left(\frac{1}{\zeta_{2j} - \zeta'_{2j}} \right)$$

$$+ 2\pi\rho\kappa_1\kappa_2 \left(\frac{1}{\zeta_{1j} - \zeta'_{2j}} + \frac{1}{\zeta_{2j} - \zeta'_{1j}} \right) - 2\pi\rho\kappa_0 \left(\frac{\kappa_1}{\zeta_{1j}} + \frac{\kappa_2}{\zeta_{2j}} \right)$$

$$- 2\pi\rho u_0 \left(\kappa_1 \left(\frac{a^2}{\zeta_{1j}^2} + 1 \right) + \kappa_2 \left(\frac{a^2}{\zeta_{2j}^2} + 1 \right) - \kappa_0 \right). \qquad (2.68)$$

We see that when the vortices have same strength ($\kappa_1 = \kappa_2$), force is never zero. If $\kappa_1 = -\kappa_2$ then for force to be zero vortices must be placed symmetrically with respect to the centre of the cylinder and $\kappa_0 = 0$.

Notice that the circulation around the cylinder depends on the value of κ_0

$$
\begin{aligned}
\Gamma &= Re\left(\int_{|\zeta_j|=a} i\kappa_1 \left(\frac{1}{\zeta_j - \zeta_{1j}} - \frac{1}{\zeta_j - \zeta'_{1j}}\right) dz\right) \\
&\quad + Re\left(\int_{|\zeta_j|=a} i\kappa_0 \left(\frac{1}{\zeta_j}\right) dz\right) + Re\left(\int_{|\zeta_j|=a} iu_0 \left(1 + \frac{a^2}{\zeta_j^2}\right) dz\right) \\
&\quad + Re\left(\int_{|\zeta_j|=a} i\kappa_2 \left(\frac{1}{\zeta_j - \zeta_{2j}} - \frac{1}{\zeta_j - \zeta'_{2j}}\right) dz\right) \\
&= 2\pi(\kappa_1 + \kappa_2 - \kappa_0),
\end{aligned}
\tag{2.69}
$$

when $\kappa_0 = \kappa_1 + \kappa_2$, circulation would be zero, as expected.

2.6. Flow around N-Cylinders and M-Vortices

Now we assume that there are N cylinders of radii $a_1, ... a_N$ placed at points $z_1, ..., z_N$ and that M vortices are placed at points $z_{01}, ..., z_{0m}$ outside the cylinders with strengths of $\kappa_1, ..., \kappa_m$ respectively. Then the velocity field is given as

$$
\overline{V}_j^T = \overline{V}_j^I + \overline{V}_j^D + \sum_{\substack{i=1 \\ i\neq j}}^{N} \overline{V}_i^D,
\tag{2.70}
$$

where

$$
\overline{V}_j^I = -\sum_{m=1}^{M}\left(\frac{i\kappa_m}{\zeta_{mj}}\sum_{n=0}^{\infty}\left(\frac{\zeta_j}{\zeta_{mj}}\right)^n\right) \;,\; |\zeta_j| < |\zeta_{mj}|,
\tag{2.71}
$$

$$
\overline{V}_j^D = -\sum_{m=1}^{M}\left(i\kappa_m \sum_{n=1}^{\infty} A_n^j \frac{(\zeta'_{mj})^n}{\zeta_j^{n+1}}\right) \;,\; |\zeta'_{mj}| \leq |\zeta_j|,
\tag{2.72}
$$

$$
\overline{V}_i^D = -\sum_{m=1}^{M}\left(i\kappa_m \sum_{n=1}^{\infty} A_n^i \frac{(\zeta'_{mi})^n}{\zeta_i^{n+1}}\right) = -\sum_{m=1}^{M}\left(i\kappa_m \sum_{n=1}^{\infty} A_n^i \frac{(\zeta'_{mi})^n}{(\zeta_j + R_{ij})^{n+1}}\right)
\tag{2.73}
$$

and A_n^i are unknown complex coefficients. We see that for the case of a single cylinder the unknown coefficient A_n^j in (4) becomes unity.

The boundary condition to be satisfied for each cylinder is that "the normal component of $\overline{V}_j^T = 0$, when $|\zeta_j| = a_j, \forall j$". This condition is equivalent to the statement

$$a_j Re(\overline{V}_j^T e^{i\theta_j}) = Re(\overline{V}_j^T a_j e^{i\theta_j}) = Re(\overline{V}_j^T \zeta_j) = 0, \ \ j = 1, ..., N. \qquad (2.74)$$

Application of this condition yields

$$Re\left(\sum_{m=1}^{M}\left(i\kappa_m\left(\sum_{n=0}^{\infty}\frac{\zeta_j^{n+1}}{\zeta_{mj}^{n+1}} + \sum_{n=1}^{\infty}\frac{B_{nm}^j}{\zeta_j^n} + \sum_{i=1}^{N}(1-\delta_{ij})\sum_{n=1}^{\infty}\frac{B_{nm}^i\zeta_j}{(\zeta_j + Rij)^{n+1}}\right)\right)\right) = 0,$$

$$\qquad (2.75)$$

where $B_{nm}^j = A_n^j\dfrac{a_j^{2n}}{\zeta_{mj}^n}$ and $\delta_{ij} = 1$ when $i = j$, $\delta_{ij} = 0$ otherwise.

The last term in (2.75) must be expanded into a series

$$\frac{1}{(\zeta_j + R_{ij})^{n+1}} = \frac{1}{R_{ij}^{n+1}}\sum_{k=0}^{\infty}\frac{(n+1)_k}{k!}\left(-\frac{\zeta_j}{R_{ij}}\right)^k, \qquad (2.76)$$

where $(n+1)_k = (n+1)(n+2)...(n+k)$ is the Pochhammer symbol and $(n+1)_0 = 1$. Equation (2.75) is equivalent to

$$i\left(\sum_{m=1}^{M}\left(\kappa_m\left(\sum_{n=0}^{\infty}\frac{\zeta_j^{n+1}}{\zeta_{mj}^{n+1}} + \sum_{n=1}^{\infty}\frac{B_{nm}^j}{\zeta_j^n}\right.\right.\right.$$

$$\left.\left.\left. + \sum_{i=1}^{N}(1-\delta_{ij})\sum_{n=1}^{\infty}\frac{B_{nm}^i\zeta_j}{(Rij)^{n+1}}\sum_{k=0}^{\infty}\frac{(n+1)_k}{k!}\left(\frac{-\zeta_j}{R_{ij}}\right)^k\right)\right)\right) + c.c. = 0,$$

$$\qquad (2.77)$$

when $|\zeta_j| = a_j$, where $c.c.$ stands for the complex conjugation. Using $\zeta_j\overline{\zeta}_j = a^2$ in (2.77) leads to

31

$$\sum_{m=1}^{M} \left(\sum_{n=0}^{\infty} \left(\frac{\zeta_j}{\zeta_{mj}} \right)^{n+1} - \sum_{n=1}^{\infty} \frac{\zeta_j^n \overline{B}_n^j}{a_j^{2n}} \right.$$

$$\left. + \sum_{i=1}^{N} (1 - \delta_{ij}) \sum_{n=1}^{\infty} \frac{B_{nm}^i}{R_{ij}^{n+1}} \sum_{k=0}^{\infty} (-1)^k \frac{(n+1)_k}{k!} \frac{\zeta_j^{k+1}}{R_{ij}^k} \right) = 0. \quad (2.78)$$

Equating every coefficient for all n and for all m we have an algebraic system for the unknown coefficients B_{lm}^s

$$\sum_{l=1}^{\infty} \sum_{s=1}^{N} D_{nl}^{js} B_{lm}^s = C_{nm}^j, \quad j = 1, ..., N, \quad m = 1, ..., M, \quad n = 0, 1, ... \quad (2.79)$$

where

$$\begin{aligned} D_{nl}^{js} &= -\frac{\delta_{n+1,l} \delta_{j,s}}{a_j^{2n+2}} + \frac{(-1)^n}{n!} \sum_{k=1}^{\infty} \sum_{i=1}^{N} (1 - \delta_{si})(1 - \delta_{ij}) \\ &\quad \times \frac{(-1)^{k-1}}{(k-1)!} \frac{a_i^{2k} (k+1)_n (l+1)_{k-1}}{R_{si}^{k+l} \overline{R}_{ij}^{n+k+1}}, \end{aligned} \quad (2.80)$$

$$C_{nm}^j = \frac{-1}{\overline{\zeta}_{mj}^{n+1}} - \frac{(-1)^n}{n!} \sum_{i=1}^{N} (1 - \delta_{ij}) \sum_{k=1}^{\infty} \frac{(k+1)_n a_i^{2k}}{\overline{R}_{ij}^{n+k+1}} \frac{1}{\zeta_{mi}^k}. \quad (2.81)$$

The only difference in the formulations of one vortex-N cylinder and M vortex-N cylinder is that in the latter the infinite by infinite algebraic system (2.79) should be solved for every vortex m.

As an example consider the case of two vortices with the same strength $\kappa_1 = \kappa_2 = 0.4$, at the points $z_{01} = -2 + 3i$, $z_{02} = -3i$ and the cylinders at the points $\zeta_1 = -2$, $\zeta_2 = 2$ then velocity field can be shown as in Figure 2.14. We observe that the slip boundary condition is satisfied.

In another example consider the case of two vortices with strengths $\kappa_1 = 0.4$,
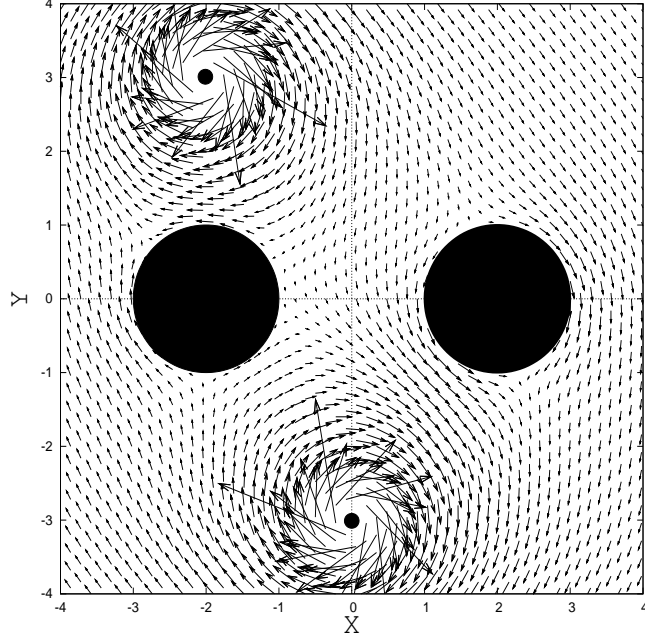
Figure 2.14. Velocity distribution about two cylinders at the points $(-2, 0)$ and $(2, 0)$ with two vortices of same strength $\kappa_1 = \kappa_2 = 0.4$ at the points $(0, -3)$ and $(-2, 3)$. Velocity vectors are scaled down by the factor of 1.3.

$\kappa_2 = -0.4$ at the points $z_{01} = 3i$, $z_{02} = -3i$ and the cylinders at the points $\zeta_1 = 2 + 2i$, $\zeta_2 = -2 + 2i$, $\zeta_3 = -2 - 2i$, $\zeta_4 = 2 - 2i$ then velocity field can be shown as in Figure 2.15. This configuration resembles the legs of the TLP with two vortices.

For the M vortex case by Blasius' Theorem, the force on the system is given by

$$
\begin{aligned}
\overline{F} &= \frac{i\rho}{2} \int\limits_{|\zeta_j|=a_j} \left(\overline{V}_j^T\right)^2 d\zeta_j \\
&= \sum_{p=1}^{M} \sum_{r=1}^{M} \left(\frac{2\pi\rho\kappa_p\kappa_r}{\zeta_{pj}} \left(\sum_{n=1}^{\infty} \frac{A_n^j (\zeta'_{rj})^n}{\zeta_{pj}^n} \right) \right) \\
&\quad + \sum_{p=1}^{M} \sum_{r=1}^{M} \left(2\pi\rho\kappa_p\kappa_r \sum_{n=1}^{\infty} \sum_{m=1}^{\infty} (-1)^n A_n^j A_m^i \frac{(\zeta'_{pj})^n (\zeta'_{ri})^m}{(R_{ij})^{m+n+1}} \frac{(n+1)_n}{n!} \right). \quad (2.82)
\end{aligned}
$$

We can verify the above formula (2.82) by reducing it to the case of one cylinder and two vortices case and compare it by the formula (2.56). Since we have one cylinder all coefficients A_n^j become unity and the term $\overline{V}_i^D$ become zero. Since $|\zeta'_{pj}| < |\zeta_{rj}|\ \forall p, r$, $\overline{F}$ becomes

33
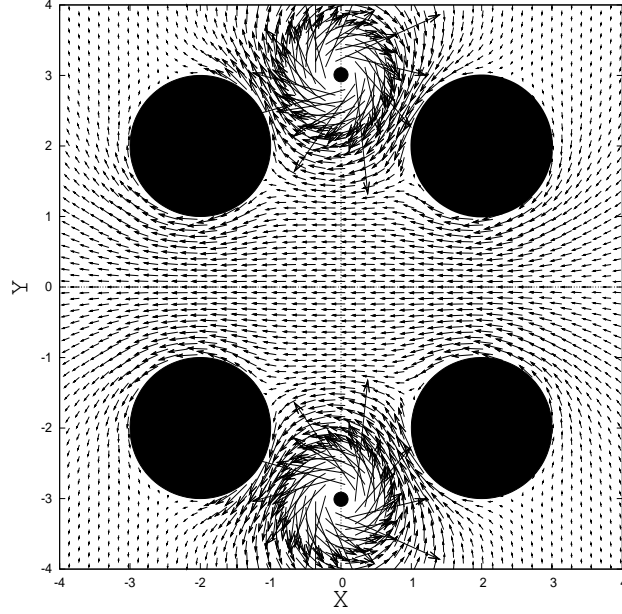
Figure 2.15. Velocity distribution about four cylinders at the points $(2, 2)$, $(-2, 2)$, $(-2, -2)$ and $(2, -2)$ with two vortices of vanishing total strength $\kappa_1 = -\kappa_2 = 0.4$ at the points $(0, 3)$ and $(0, -3)$. Velocity vectors are scaled down by the factor of 1.3.

$$
\begin{aligned}
\overline{F} &= \frac{2\pi\rho\kappa_1^2}{\zeta_{1j}} \sum_{n=1}^{\infty} \frac{(\zeta'_{1j})^n}{\zeta_{1j}^n} + \frac{2\pi\rho\kappa_2^2}{\zeta_{2j}} \sum_{n=1}^{\infty} \frac{(\zeta'_{2j})^n}{\zeta_{2j}^n} \\[2mm]
&\quad + \frac{2\pi\rho\kappa_1\kappa_2}{\zeta_{1j}} \sum_{n=1}^{\infty} \frac{(\zeta'_{2j})^n}{\zeta_{1j}^n} + \frac{2\pi\rho\kappa_1\kappa_2}{\zeta_{2j}} \sum_{n=1}^{\infty} \frac{(\zeta'_{1j})^n}{\zeta_{2j}^n} \\[2mm]
&= \frac{2\pi\rho\kappa_1^2}{\zeta_{1j}} \left(\frac{\zeta_{1j}}{\zeta_{1j} - \zeta'_{1j}} - 1 \right) + \frac{2\pi\rho\kappa_2^2}{\zeta_{2j}} \left(\frac{\zeta_{2j}}{\zeta_{2j} - \zeta'_{2j}} - 1 \right) \\[2mm]
&\quad + \frac{2\pi\rho\kappa_1\kappa_2}{\zeta_{1j}} \left(\frac{\zeta_{1j}}{\zeta_{1j} - \zeta'_{2j}} - 1 \right) + \frac{2\pi\rho\kappa_1\kappa_2}{\zeta_{2j}} \left(\frac{\zeta_{2j}}{\zeta_{2j} - \zeta'_{1j}} - 1 \right) \\[2mm]
&= 2\pi\rho\kappa_1^2 \left(\frac{1}{\zeta_{1j} - \zeta'_{1j}} - \frac{1}{\zeta_{1j}} \right) + 2\pi\rho\kappa_2^2 \left(\frac{1}{\zeta_{2j} - \zeta'_{2j}} - \frac{1}{\zeta_{2j}} \right) \\[2mm]
&\quad + 2\pi\rho\kappa_1\kappa_2 \left(\frac{1}{\zeta_{1j} - \zeta'_{2j}} + \frac{1}{\zeta_{2j} - \zeta'_{1j}} - \frac{1}{\zeta_{1j}} - \frac{1}{\zeta_{2j}} \right),
\end{aligned}
\tag{2.83}
$$

34

which is the same result as in the equation (2.56).

And using Cauchy's Theorem we can calculate the circulation around the j-th cylinder

$$\Gamma \;=\; Re\left(\oint_{|\zeta_j|=a_j} \overline{V}_j^{T} d\zeta_j\right) = Re\left(\oint_{|\zeta_j|=a_j} \left(\overline{V}_j^{I} + \overline{V}_j^{D} + \sum_{\substack{i=1 \\ i\neq j}}^{N} \overline{V}_i^{D}\right) d\zeta_j\right) = 0.$$

(2.84)

CHAPTER 3

MOTION OF VORTICES

3.1. Hamiltonian Dynamics

In order to integrate a system of $2n$ ordinary differential equations, we must know $2n$ first integrals. It turns out that if we are given a canonical system of differential equations, it is often sufficient to know only n first integrals, each of them allows us to reduce the order of the system not just by one, but by two.

We will give necessary background to learn about the Hamiltonian formulation which provides natural framework in which to investigate the integrability of the system (Newton 2000). Let us recall that a $2n$-dimensional vector field is said to be Hamiltonian if the associated flow satisfies a system of ordinary differential equations of the form

$$\dot{q} = \frac{\partial H}{\partial p}, \quad \dot{p} = -\frac{\partial H}{\partial q}, \tag{3.1}$$

where the variable $p = (p_1, ..., p_n)$ is called the momentum and $q = (q_1, ..., q_n)$ is called the position. The function $H : (t, q, p) \in G \subset \mathbb{R} \times \mathbb{R}^{2n} \rightarrow H(t, q, p) \in \mathbb{R}$ where G is some open set of $\mathbb{R} \times \mathbb{R}^{2n}$, is called the Hamiltonian of the system (3.1) and the equations are known as the Hamilton equations. The variables q and p are said to be conjugate variables, p is conjugate to q, etc. The integer n is the number of degrees of freedom of the system and Hamiltonian is said to have n degrees of freedom. The notion of "degrees of freedom" as it is used for Hamiltonian systems means one canonical conjugate pair, for example, the position, q, and its conjugate momentum, p. Hamiltonian systems always have such pairs of variables, and so the phase space which is the collection of possible states of a dynamical system is even dimensional.

For the general discussion, introduce the $2n$ vector z and the $2n \times 2n$ skew symmetric matrix J and the gradient by

$$z = \begin{pmatrix} q \\ p \end{pmatrix}, \quad J = \begin{pmatrix} 0 & I \\ -I & 0 \end{pmatrix}, \quad \nabla_z = \nabla H = \begin{pmatrix} \dfrac{\partial H}{\partial z_1} \\ \vdots \\ \dfrac{\partial H}{\partial z_{2n}} \end{pmatrix},$$

where 0 is the $n \times n$ zero matrix and I is the $n \times n$ identity matrix. In this notation the equation (3.1) becomes

$$\dot{z} = J \nabla H(t, z). \tag{3.2}$$

By the existence and uniqueness theorem (Newton 2000), for continuously differentiable H and for each $(t_0, z_0) \in G$, there is a unique solution $z = \phi(t, t_0, z_0)$ of (3.2) defined for t near t_0 which satisfies the initial condition $\phi(t_0, t_0, z_0) = z_0$. ϕ is defined on an open neighbourhood of the set $\{(t, t_0, z) \in G : t = t_0\}$ into $\mathbb{R}^n$. The function $\phi(t, t_0, z_0)$ is called the general solution.

In the special case when H is independent of t, $H : G \to \mathbb{R}$ where G is the some open set in $\mathbb{R}^{2n}$, the differential equations (3.2) are autonomous and the Hamiltonian system is called conservative. In this case the identity $\phi(t - t_0, 0, z_0) = \phi(t, t_0, z_0)$ holds, since both sides satisfy equation (3.2) and the same initial conditions. In this case usually t_0 dependence is dropped and only $\phi(t, z_0)$ is considered, where $\phi(t, z_0)$ is the solution of (3.2) satisfying $\phi(0, z_0) = z_0$. The solutions are pictured as parameterized curves in $G \subset \mathbb{R}^{2n}$ and the set G is called the phase space. By the existence and uniqueness theorem (Newton 2000), there is a unique curve through each point and two such solution curves cannot cross in G.

An integral for (3.2) is a smooth function $f : G \to \mathbb{R}$ which is constant along the solutions of (3.2), i.e., $f(\phi(t, z_0)) = f(z_0)$ is constant. The classical conserved quantities of energy, momentum, etc., are integrals. The level surfaces $f^{-1}(c) \subset \mathbb{R}^{2n}$, where c is a constant, are invariant sets, i.e., if a solution starts in the set, it remains in the set. We will give the conditions for the integrability of the system after some definitions.

Now consider the time derivative of a C^1 function $f(t, q, p)$ defined on the $2n$-dimensional phase space. By the chain rule

$$
\begin{aligned}
\frac{df}{dt} &= \sum_{i=1}^{n} \left(\frac{\partial f}{\partial q_i} \frac{\partial q_i}{\partial t} + \frac{\partial f}{\partial p_i} \frac{\partial p_i}{\partial t} \right) + \frac{\partial f}{\partial t} \\
&= \sum_{i=1}^{n} \left(\frac{\partial f}{\partial q_i} \frac{\partial H}{\partial p_i} + \frac{\partial f}{\partial p_i} \frac{\partial H}{\partial q_i} \right) + \frac{\partial f}{\partial t} \\
&= \{f, H\} + \frac{\partial f}{\partial t}.
\end{aligned}
\tag{3.3}
$$

The last step defines the canonical Poisson bracket of two functions

$$\{f, g\} = \sum_{i=1}^{n} \left(\frac{\partial f}{\partial q_i} \frac{\partial g}{\partial p_i} + \frac{\partial f}{\partial p_i} \frac{\partial g}{\partial q_i} \right). \tag{3.4}$$

The formula (3.3) shows that if the function f is time independent and if its Poisson bracket with the Hamiltonian vanishes, then it is a conserved quantity or integral for (3.2) and also shows that H is an integral for (3.2) and $\{f, H\}$ is the time rate of change of f along the solutions of (3.2). Two functions whose Poisson bracket vanishes are said to be involutive or in involution. Equivalently, they are said to Poisson commute.

We can now define the notion of complete integrability for a Hamiltonian system based on the number of conserved quantities, or symmetry groups of the system:

Definition 3.1.0.1 *In a Hamiltonian system with n degrees of freedom (2n-dimensional phase space) and $k \leq n$ functionally independent involutive conserved quantities, one can reduce the dimension of the phase space to (2n-k). If k=n, the system is said to be completely integrable and in principle can be solved by quadrature.*

In the Hamiltonian description there are two sets of independent variables, the p_i and q_i $(i = 1, ..., n)$. It is sometimes convenient to transform to some new set of generalized coordinates (e.g., a transformation from cartesian to polar coordinates), from one set of phase space variables (p_i, q_i) to some new set (P_i, Q_i), that is,

$$P_i = P_i(q_1, ..., q_n, p_1, ..., p_n) \tag{3.5}$$

$$Q_i = P_i(q_1, ..., q_n, p_1, ..., p_n). \tag{3.6}$$

where canonical form of Hamilton's equations are still preserved

$$\dot{Q}_i = \frac{\partial}{\partial P_i} H'(Q, P), \quad \dot{P}_i = -\frac{\partial}{\partial Q_i} H'(Q, P), \tag{3.7}$$

where $H' = H'(Q(q, p), P(q, p))$ is the transformed Hamiltonian. These transformations are called the canonical transformations.

The practical use of canonical transformations is to find those transformations that make the integration of Hamilton's equations as simple as possible. The optimal case is

the one in which all the Q_i are cyclic; that is, the transformed Hamiltonian depends only on the new momenta P_i

$$H(q_1, ..., q_n, p_1, ..., p_n) \to H'(P_1, ..., P_n,),\tag{3.8}$$

then Hamilton's equations become very simple,

$$
\begin{aligned}
\dot{P}_i &= -\frac{\partial H'}{\partial Q_i} H' = 0, \quad i.e., \ P_i = \text{constant}, \quad i = 1, ..., n \\
\dot{Q}_i &= \frac{\partial H'}{\partial P_i} = f_i(P_1, ..., P_n)
\end{aligned}\tag{3.9}
$$

where the f_i are some time independent function of the P_i. In this case the Hamiltonian system is called to be completely integrable.

3.2. Hamiltonian Description of Motion of Vortices

In previous chapter we have considered the fluid advection problems of vortices and a uniform flow in the presence of cylinder(s) and also considered the velocity distributions at fixed moment of time. Now we shall observe the motion of the vortices in the time domain in which the vortices are allowed to move with the flow and try to integrate the system.

3.2.1. Motion of a Vortex around a Cylinder

We start with a simple system. Consider a vortex of strength κ placed at z_0 and a cylinder of radius a at the origin. The complex velocity is

$$\overline{V} = \frac{i\kappa}{z - z_0} - \frac{i\kappa}{z - z_0'} + \frac{i\kappa}{z} \ , \ \ z = x + iy,\tag{3.10}$$

which is defined by the equation (2.18) and the motion equation of the vortex is

$$\frac{d\overline{z}}{dt} = \frac{dx}{dt} - i\frac{dy}{dt} = \frac{i\kappa}{z - z_0} - \frac{i\kappa}{z - \dfrac{a^2}{\overline{z}_0}} + \frac{i\kappa}{z}. \qquad (3.11)$$

Motion of the vortex at z_0 can be found by replacing z by z_0 in equation (3.11) and omitting the effect of the vortex itself (vortex cannot move itself)

$$\frac{d\overline{z}_0}{dt} = -\frac{i\kappa}{z_0 - \dfrac{a^2}{\overline{z}_0}} + \frac{i\kappa}{z_0} = -\frac{i\kappa\overline{z}_0}{|z_0|^2 - a^2} + \frac{i\kappa\overline{z}_0}{|z_0|^2}. \qquad (3.12)$$

Letting $z_0 = x_0 + iy_0$ in equation (3.12) we get

$$\frac{1}{\kappa}\frac{dx_0}{dt} = \frac{-a^2 y_0}{(x_0^2 + y_0^2)(x_0^2 + y_0^2 - a^2)},$$

$$-\frac{1}{\kappa}\frac{dy_0}{dt} = \frac{-a^2 x_0}{(x_0^2 + y_0^2)(x_0^2 + y_0^2 - a^2)}.$$

$$\begin{aligned} \frac{1}{\kappa}\frac{d\overline{z}_0}{dt} &= \frac{-a^2(y_0 + ix_0)}{(x_0^2 + y_0^2)(x_0^2 + y_0^2 - a^2)} = \frac{-a^2 i(x_0 - iy_0)}{z_0\overline{z}_0(z_0\overline{z}_0 - a^2)} \\ &= \frac{-a^2 i}{z_0(z_0\overline{z}_0 - a^2)}. \end{aligned} \qquad (3.13)$$

We can rewrite the equation (3.13) as follows

$$\frac{1}{\kappa}\left(z_0\frac{d\overline{z}_0}{dt}\right) = \frac{-a^2 i}{z_0\overline{z}_0 - a^2} \quad , \quad \frac{1}{\kappa}\left(\overline{z}_0\frac{dz_0}{dt}\right) = \frac{a^2 i}{z_0\overline{z}_0 - a^2},$$

$$\frac{d(z_0\overline{z}_0)}{dt} = 0. \qquad (3.14)$$

Thus $|\overline{z}_0|^2 = $ constant. Letting $z_0(t) = re^{i\theta(t)}$ and $z_0(0) = re^{i\theta(0)}$ we have the initial value problem

$$\frac{1}{\kappa}r^2\theta' = \frac{a^2}{r^2 - a^2} \quad , \quad \theta(0) = \theta_0 \tag{3.15}$$

and the solution is

$$z_0(t) = re^{iwt}, \tag{3.16}$$

where $w = \dfrac{a^2/r^2\kappa}{r^2 - a^2} + \theta_0$ is frequency.

The trajectory of motion of a vortex around a cylinder is shown in Figure 3.1 for different values of $z_0(0)$. We see that the streamlines are concentric circles with center at the origin.
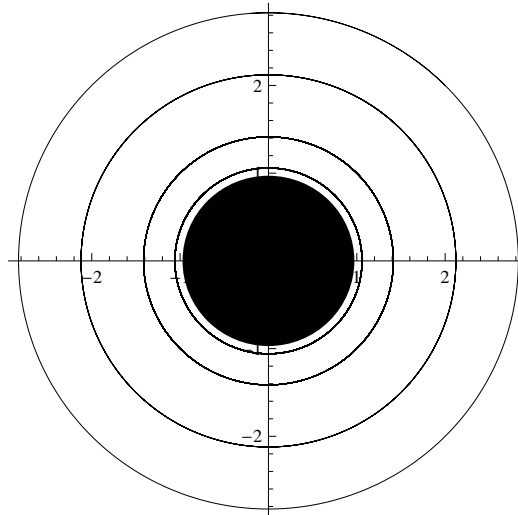
Figure 3.1. Trajectory of motion of a vortex around single cylinder.

Consider the function

$$H = \frac{a^2\kappa}{2}\left(\log\left(x_0^2 + y_0^2\right) - \log\left(x_0^2 + y_0^2 - a^2\right)\right). \tag{3.17}$$

Then we see that it satisfies the Hamiltonian equations for the vortex motion

$$\frac{dx_0}{dt} = \frac{\partial H}{\partial y_0},$$

$$\frac{dy_0}{dt} = -\frac{\partial H}{\partial x_0}. \tag{3.18}$$

Hence the system is Hamiltonian and we have one degree of freedom. It is easy to see that $\{H, H\} = 0$. The system of one vortex and single cylinder is completely integrable according to definition (3.1.0.1). The phase portrait of equations (3.18) is obtained by the level curves of H which is shown in the Figure 3.2.
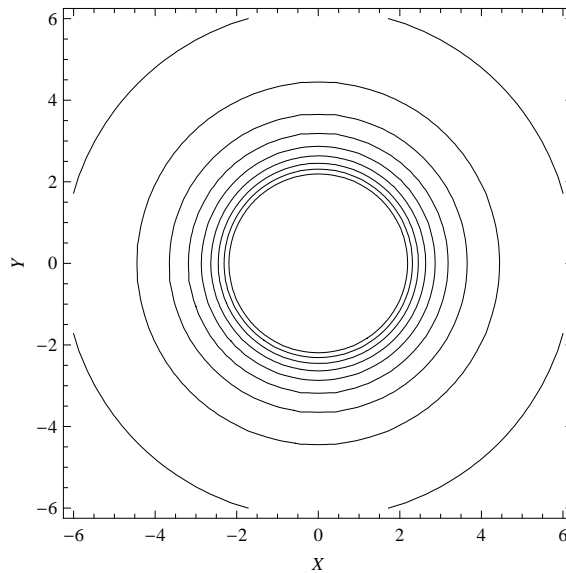
Figure 3.2. Level curves for one vortex around single cylinder.

3.2.2. Motion of a Vortex around N-Cylinders

Consider a vortex of strength κ placed at z_0 and N cylinders of radii $a_1, ...a_N$ placed at points $z_1, ..., z_N$. The complex velocity is

$$\overline{V}_j^T = \overline{V}_j^I + \overline{V}_j^D + \sum_{\substack{i=1 \\ i\neq j}}^{N} \overline{V}_i^D,$$

which is defined in the equation (2.32).

The motion of vortex at z_0 can be found using the differential equation

$$\frac{d\overline{z}_0}{dt} = -i\kappa \sum_{j=1}^{N} \sum_{n=1}^{\infty} A_n^j \frac{\left(\zeta_{0j}'\right)^n}{\zeta_j^{n+1}} = -i\kappa \sum_{j=1}^{N} \sum_{n=1}^{\infty} \frac{A_n^j}{\zeta_j} \left(\frac{a_j}{|\zeta_{0j}|}\right)^{2n}. \tag{3.19}$$

Letting $z_0 = x_0 + iy_0$ we have a system of nonlinear differential equations

$$\frac{dx_0}{dt} = \kappa \sum_{j=1}^{N} \sum_{n=1}^{\infty} \frac{a_j^{2n}}{|\zeta_{0j}|^{2n+2}} \left(Im(A_n^j)Re(\zeta_{0j}) - Re(A_n^j)Im(\zeta_{0j})\right), \tag{3.20}$$

$$\frac{dy_0}{dt} = \kappa \sum_{j=1}^{N} \sum_{n=1}^{\infty} \frac{a_j^{2n}}{|\zeta_{0j}|^{2n+2}} \left(Re(A_n^j)Im(\zeta_{0j}) + Im(A_n^j)Re(\zeta_{0j})\right). \tag{3.21}$$

The trajectory of motion of a vortex around two cylinders is shown in Figure 3.3, which is also given by Johnson and McDonald for cylinders of differing radii. The trajectory of motion of a vortex around four cylinders placed at the vertices of a square is interesting (see Figure 3.4). We notice that the centre of the geometry is a stable centre point, whereas for two cylinders, the midpoint of the cylinders is a saddle point (unstable). In both configurations, if the vortex is close enough to one of the cylinders, it will rotate around that cylinder. In other words, the centre of any cylinder is a centre point.
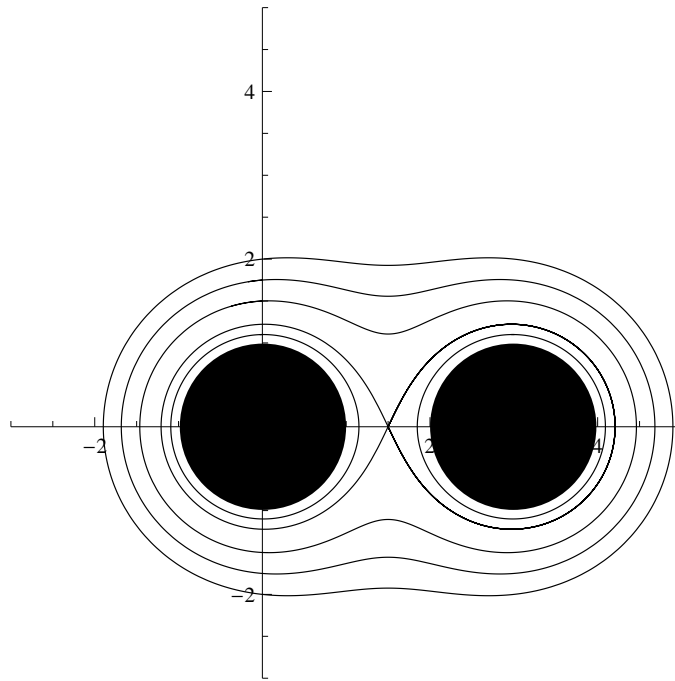
Figure 3.3. Trajectory of motion of a vortex around two cylinders.
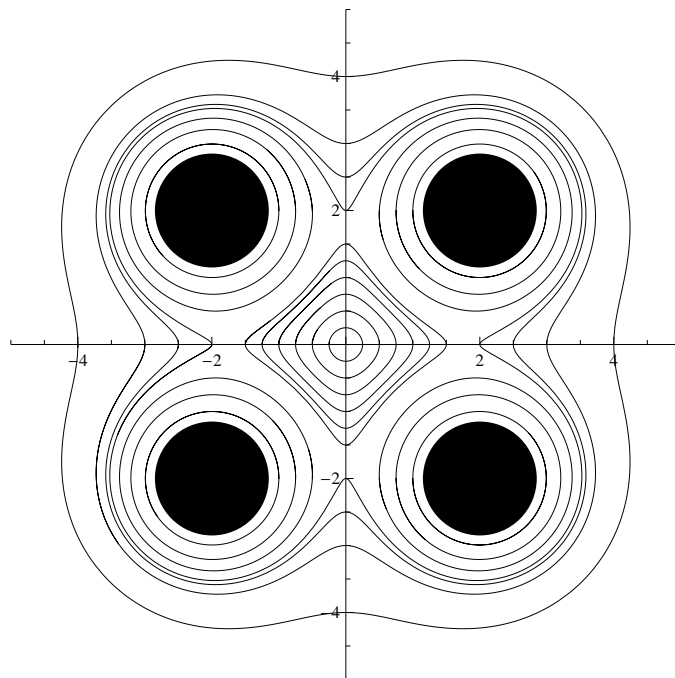
Figure 3.4. Trajectory of motion of a vortex around four cylinders.

3.2.3. Motion of Two Vortices around a Cylinder

Consider two vortices of strengths κ_1, κ_2 at z_{01}, z_{02} and a cylinder of radius a at the origin (Tülü & Yilmaz 2010). Using equation (2.54), the generalized complex velocity is given by

$$\overline{V} = \frac{i\kappa_1}{z - z_{01}} - \frac{i\kappa_1}{z - \frac{a^2}{\overline{z}_{01}}} + \frac{i\kappa_2}{z - z_{02}} - \frac{i\kappa_2}{z - \frac{a^2}{\overline{z}_{02}}} + \frac{i\kappa_0}{z}. \tag{3.22}$$

The motion of vortex at z_{01} can be found by replacing z by z_{01} in (3.22) and omitting the effect of the vortex itself

$$\frac{d\overline{z}_{01}}{dt} = \frac{i\kappa_2}{z_{01} - z_{02}} - \frac{i\kappa_1\overline{z}_{01}}{|z_{01}|^2 - a^2} - \frac{i\kappa_2\overline{z}_{02}}{z_{01}\overline{z}_{02} - a^2} + \frac{i\kappa_0}{z_{01}}. \tag{3.23}$$

The motion of vortex at z_{02} can be found similarly

$$\frac{d\overline{z}_{02}}{dt} = \frac{i\kappa_1}{z_{02} - z_{01}} - \frac{i\kappa_2\overline{z}_{02}}{|z_{02}|^2 - a^2} - \frac{i\kappa_1\overline{z}_{01}}{z_{02}\overline{z}_{01} - a^2} + \frac{i\kappa_0}{z_{02}}. \tag{3.24}$$

Letting $z_{01} = x_{01} + iy_{01}$ and $z_{02} = x_{02} + iy_{02}$ we have a system of four coupled ordinary nonlinear differential equations

$$
\begin{aligned}
\frac{dx_{01}}{dt} &= \frac{\kappa_2(y_{01} - y_{02})}{(x_{01} - x_{02})^2 + (y_{01} - y_{02})^2} - \frac{\kappa_1 y_{01}}{x_{01}^2 + y_{01}^2 - a^2} + \frac{\kappa_0 y_{01}}{x_{01}^2 + y_{01}^2} \\
&\quad + \frac{\kappa_2(a^2 y_{02} - y_{01}x_{02}^2 - y_{01}y_{02}^2)}{(a^2 - x_{01}x_{02} - y_{01}y_{02})^2 + (y_{01}x_{02} - x_{01}y_{02})^2} \\
&= \frac{\kappa_2(y_{01} - y_{02})}{|z_{01} - z_{02}|^2} - \frac{\kappa_1 y_{01}}{|z_{01}|^2 - a^2} + \frac{\kappa_0 y_{01}}{|z_{01}|^2} + \frac{\kappa_2(a^2 y_{02} - y_{01}|z_{02}|^2)}{|z_{01}\overline{z}_{02} - a^2|^2}, \tag{3.25}
\end{aligned}
$$

$$\frac{dy_{01}}{dt} = -\frac{\kappa_2(x_{01} - x_{02})}{(x_{01} - x_{02})^2 + (y_{01} - y_{02})^2} + \frac{\kappa_1 x_{01}}{x_{01}^2 + y_{01}^2 - a^2} - \frac{\kappa_0 x_{01}}{x_{01}^2 + y_{01}^2}$$

$$-\frac{\kappa_2(a^2 x_{02} - x_{01} y_{02}^2 - x_{01} x_{02}^2)}{(a^2 - x_{01} x_{02} - y_{01} y_{02})^2 + (y_{01} x_{02} - x_{01} y_{02})^2}$$

$$= -\frac{\kappa_2(x_{01} - x_{02})}{|z_{01} - z_{02}|^2} + \frac{\kappa_1 x_{01}}{|z_{01}|^2 - a^2} - \frac{\kappa_0 x_{01}}{|z_{01}|^2} - \frac{\kappa_2(a^2 x_{02} - x_{01}|z_{02}|^2)}{|z_{01}\overline{z}_{02} - a^2|^2}, (3.26)$$

$$\frac{dx_{02}}{dt} = \frac{\kappa_1(y_{02} - y_{01})}{(x_{02} - x_{01})^2 + (y_{02} - y_{01})^2} - \frac{\kappa_2 y_{02}}{x_{02}^2 + y_{02}^2 - a^2} + \frac{\kappa_0 y_{02}}{x_{02}^2 + y_{02}^2}$$

$$+\frac{\kappa_1(a^2 y_{01} - y_{02} x_{01}^2 - y_{02} y_{01}^2)}{(a^2 - x_{02} x_{01} - y_{02} y_{01})^2 + (y_{02} x_{01} - x_{02} y_{01})^2}$$

$$= \frac{\kappa_1(y_{02} - y_{01})}{|z_{02} - z_{01}|^2} - \frac{\kappa_2 y_{02}}{|z_{02}|^2 - a^2} + \frac{\kappa_0 y_{02}}{|z_{02}|^2} + \frac{\kappa_1(a^2 y_{01} - y_{02}|z_{01}|^2)}{|z_{02}\overline{z}_{01} - a^2|^2}, \quad (3.27)$$

$$\frac{dy_{02}}{dt} = -\frac{\kappa_1(x_{02} - x_{01})}{(x_{02} - x_{01})^2 + (y_{02} - y_{01})^2} + \frac{\kappa_2 x_{02}}{x_{02}^2 + y_{02}^2 - a^2} - \frac{\kappa_0 x_{02}}{x_{02}^2 + y_{02}^2}$$

$$-\frac{\kappa_1(a^2 x_{01} - x_{02} y_{01}^2 - x_{02} x_{01}^2)}{(a^2 - x_{02} x_{01} - y_{02} y_{01})^2 + (y_{02} x_{01} - x_{02} y_{01})^2}$$

$$= -\frac{\kappa_1(x_{02} - x_{01})}{|z_{02} - z_{01}|^2} + \frac{\kappa_2 x_{02}}{|z_{02}|^2 - a^2} - \frac{\kappa_0 x_{02}}{|z_{02}|^2} - \frac{\kappa_1(a^2 x_{01} - x_{02}|z_{01}|^2)}{|z_{02}\overline{z}_{01} - a^2|^2}. (3.28)$$

The Hamiltonian of vortex motion easily can be written down by inspection

$$H = \frac{\kappa_1 \kappa_2}{2} \log\left((x_{01} - x_{02})^2 + (y_{01} - y_{02})^2\right) - \frac{\kappa_1^2}{2} \log\left(x_{01}^2 + y_{01}^2 - a^2\right)$$

$$-\frac{\kappa_2^2}{2} \log\left(x_{02}^2 + y_{02}^2 - a^2\right) + \frac{\kappa_1 \kappa_0}{2} \log\left(x_{01}^2 + y_{01}^2\right) + \frac{\kappa_2 \kappa_0}{2} \log\left(x_{02}^2 + y_{02}^2\right)$$

$$-\frac{\kappa_1 \kappa_2}{2} \log\left((y_{01} x_{02} - x_{01} y_{02})^2 + (y_{01} y_{02} + x_{01} x_{02} - a^2)^2\right). \tag{3.29}$$

Then it is easy to check that the motion equations can be derived using the Hamiltonian

$$\frac{dx_{0i}}{dt} = \frac{1}{\kappa_i}\frac{\partial H}{\partial y_{0i}}, \quad \frac{dy_{0i}}{dt} = -\frac{1}{\kappa_i}\frac{\partial H}{\partial x_{0i}}, \quad i = 1, 2. \tag{3.30}$$

Thus we have two degrees of freedom (4-dimensional phase space). We know that the Hamiltonian is an integral constant. We shall show that the angular momentum

$$I = \sum_{k=1}^{2} \kappa_k z_{0k}\overline{z}_{0k} \tag{3.31}$$

is also an integral constant. Since

$$\begin{aligned}
\frac{dI}{dt} &= \frac{d}{dt}\left(\sum_{k=1}^{2} \kappa_k z_{0k}\overline{z}_{0k}\right) \\
&= \kappa_1\left(2x_{01}\frac{dx_{01}}{dt} + 2y_{01}\frac{dy_{01}}{dt}\right) + \kappa_2\left(2x_{02}\frac{dx_{02}}{dt} + 2y_{02}\frac{dy_{02}}{dt}\right) = 0, \quad (3.32)
\end{aligned}$$

angular momentum is independent of time. The Poisson bracket of the Hamiltonian and the angular momentum can be calculated as follows

$$\begin{aligned}
\{I, H\} &= \frac{\partial I}{dx_{01}}\frac{\partial H}{dy_{01}} - \frac{\partial I}{dy_{01}}\frac{\partial H}{dx_{01}} + \frac{\partial I}{dx_{02}}\frac{\partial H}{dy_{02}} - \frac{\partial I}{dy_{02}}\frac{\partial H}{dx_{02}} \\
&= 2\kappa_1^2\kappa_2\frac{(x_{02}y_{02} - x_{01}y_{02})}{|z_{01} - z_{02}|^2} - 2\kappa_1^2\kappa_2\frac{(a^2y_{01}x_{02} - a^2x_{01}y_{02})}{|z_{01}\overline{z}_{02} - a^2|^2} \\
&\quad +2\kappa_1\kappa_2^2\frac{(x_{01}y_{02} - x_{02}y_{01})}{|z_{02} - z_{01}|^2} - 2\kappa_1\kappa_2^2\frac{(a^2x_{01}y_{02} - a^2x_{02}y_{01})}{|z_{01}\overline{z}_{02} - a^2|^2} \\
&= 2\kappa_1\kappa_2(\kappa_1 - \kappa_2)\frac{x_{02}y_{01}}{|z_{01} - z_{02}|^2} + 2\kappa_1\kappa_2(\kappa_2 - \kappa_1)\frac{x_{01}y_{02}}{|z_{01} - z_{02}|^2} \\
&\quad +2\kappa_1\kappa_2(\kappa_1 - \kappa_2)\frac{a^2x_{01}y_{02}}{|z_{01}\overline{z}_{02} - a^2|^2} + 2\kappa_1\kappa_2(\kappa_2 - \kappa_1)\frac{a^2x_{02}y_{01}}{|z_{01}\overline{z}_{02} - a^2|^2}.
\end{aligned}$$
$$\tag{3.33}$$

It follows from the Poisson bracket if $\kappa_1 = \kappa_2$ we obtain that $\{I, H\} = 0$ then the Hamiltonian and the angular momentum are in involution. Therefore we have two functionally independent, involutive, conserved quantities. Hence the system is integrable according to Liouville.

Next we consider three numerical examples where $\kappa_1 = \pm\kappa_2 = 1$ and $a = 1$ with different initial conditions then the motion of vortices are depicted in Figures 3.5-3.7. In Figure 3.5 we see that when the vortices have the same strength, they rotate around each other and also around the cylinder, whereas in the latter case vortices either translate with a uniform velocity (Figure 3.6) or rotate around the cylinder (Figure 3.7).
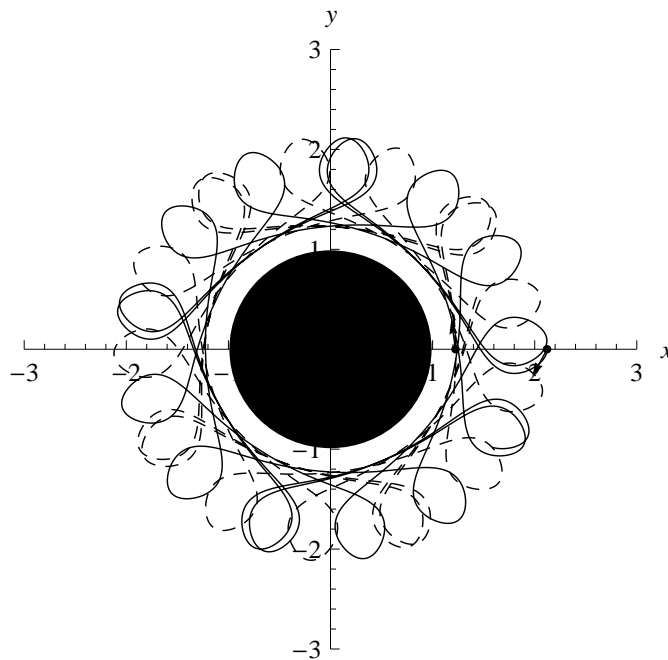
Figure 3.5. Motion of vortices of unit strength around the cylinder at the origin with initial vortex starting positions being $(1.322876, 0)$, $(2.061553, 0)$ and $\kappa_0 = \kappa_1 + \kappa_2$. Continuous and dashed lines denote the trajectories of vortices. The initial points correspond to the point B in Figure 3.8.
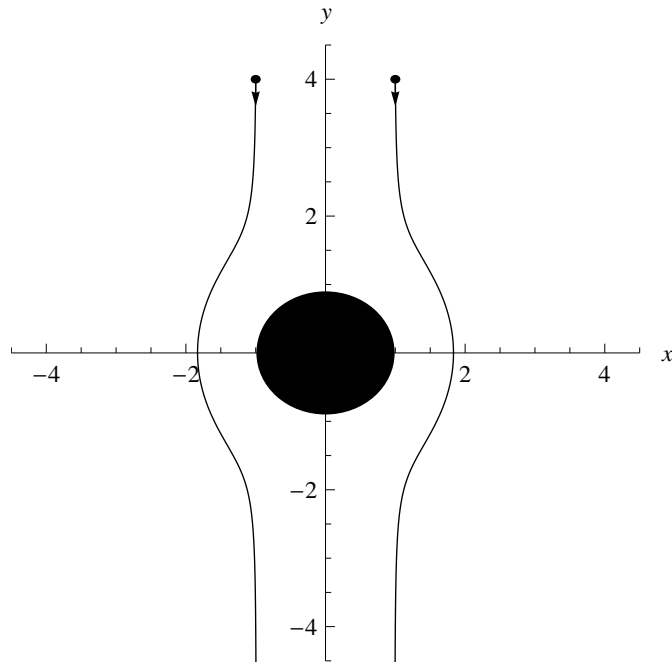
Figure 3.6. Motion of vortices with vanishing total strength around the cylinder at the origin with $\kappa_0 = \kappa_1 + \kappa_2$. Initial vortex positions are $(1, 4)$ and $(-1, 4)$.
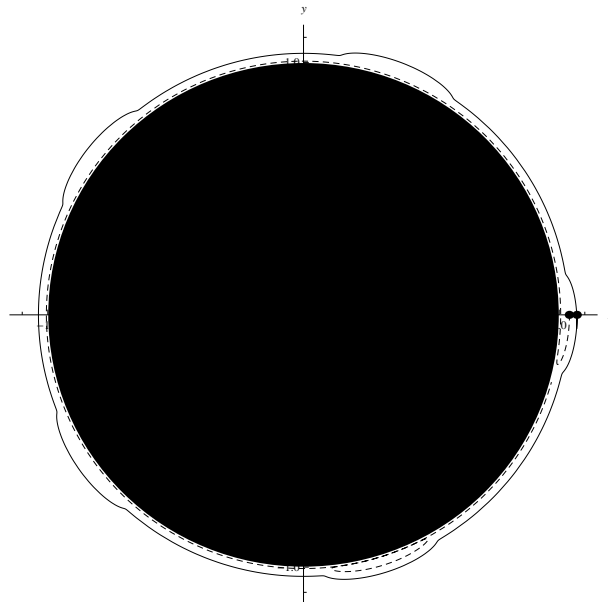
Figure 3.7. Motion of vortices with vanishing total strength around the cylinder at the origin with $\kappa_0 = \kappa_1 + \kappa_2$. Initial positions are $(1.07, 0)$ and $(1.04, 0)$. Continuous and dashed lines denote the trajectories of vortices. Small solid dots indicate the initial positions of vortices.

Since the system is integrable we shall try to reduce the system from four space variables to two space variables and then plot the constant Hamiltonian curves which gives information about the dynamical system in question. In order to put the motion equations in the usual Hamiltonian form, we let $p_i = \sqrt{|\kappa_i|} x_{0i} s_i$ and $q_i = \sqrt{|\kappa_i|} y_{0i}$ where $s_i = sign(\kappa_i)$ then we have

$$\frac{dp_i}{dt} = \frac{\partial H'}{\partial q_i}, \quad \frac{dq_i}{dt} = -\frac{\partial H'}{\partial p_{ii}}, \quad i = 1, 2. \tag{3.34}$$

where

$$
\begin{aligned}
H' &= \frac{\kappa_1 \kappa_2}{2} \log \left(\frac{p_1^2 + q_1^2}{|\kappa_1|} + \frac{p_2^2 + q_2^2}{|\kappa_2|} - \frac{2 p_1 p_2}{\sqrt{|\kappa_1 \kappa_2|} s_1 s_2} - \frac{2 q_1 q_2}{\sqrt{|\kappa_1 \kappa_2|}} \right) \\
&\quad - \frac{\kappa_1^2}{2} \log \left(\frac{p_1^2 + q_1^2}{|\kappa_1|} - a^2 \right) - \frac{\kappa_2^2}{2} \log \left(\frac{p_2^2 + q_2^2}{|\kappa_2|} - a^2 \right) \\
&\quad + \frac{\kappa_1 \kappa_0}{2} \log \left(\frac{p_1^2 + q_1^2}{|\kappa_1|} \right) + \frac{\kappa_2 \kappa_0}{2} \log \left(\frac{p_2^2 + q_2^2}{|\kappa_2|} \right) \\
&\quad - \frac{\kappa_1 \kappa_2}{2} \log \left(\frac{q_1^2 p_2^2 + p_1^2 q_2^2 + q_1^2 q_2^2 + p_1^2 p_2^2}{|\kappa_1 \kappa_2|} - 2a^2 \left(\frac{q_1 q_2}{\sqrt{|\kappa_1 \kappa_2|}} + \frac{p_1 p_2}{\sqrt{|\kappa_1 \kappa_2|} s_1 s_2} \right) + a^4 \right).
\end{aligned}
\tag{3.35}
$$

Next we employ polar coordinates $p_i^2 + q_i^2 = 2R_i$ and $q_i / p_i = \tan P_i$, $i = 1, 2$, so the Hamiltonian and the motion equations become

$$
\begin{aligned}
H'' &= \frac{\kappa_1 \kappa_2}{2} \log \left(\frac{2 R_1}{|\kappa_1|} + \frac{2 R_2}{|\kappa_2|} - \frac{4 \sqrt{R_1 R_2}}{\sqrt{|\kappa_1 \kappa_2|}} s_1 s_2 Cos(P_1 - s_1 s_2 P_2) \right) \\
&\quad - \frac{\kappa_1^2}{2} \log \left(\frac{2 R_1}{|\kappa_1|} - a^2 \right) - \frac{\kappa_2^2}{2} \log \left(\frac{2 R_2}{|\kappa_2|} - a^2 \right) \\
&\quad + \frac{\kappa_1 \kappa_0}{2} \log \left(\frac{2 R_1}{|\kappa_1|} \right) + \frac{\kappa_2 \kappa_0}{2} \log \left(\frac{2 R_2}{|\kappa_2|} \right) \\
&\quad - \frac{\kappa_1 \kappa_2}{2} \log \left(\frac{4 R_1 R_2}{|\kappa_1 \kappa_2|} - \frac{4 a^2 \sqrt{R_1 R_2}}{\sqrt{|\kappa_1 \kappa_2|}} s_1 s_2 Cos(P_1 - s_1 s_2 P_2) + a^4 \right) \tag{3.36}
\end{aligned}
$$

and

$$\frac{dR_i}{dt} = \frac{\partial H''}{\partial P_i}, \quad \frac{dP_i}{dt} = -\frac{\partial H''}{\partial R_i}, \quad i = 1, 2. \tag{3.37}$$

Finally with the new set of canonical variables

$$Q_1(P_1, P_2) = P_1 - s_1 s_s P_2 \quad , \quad Q_2(P_1, P_2) = s_2 P_2, \tag{3.38}$$

$$G_1(R_1, R_2) = R_1 \quad , \quad G_2(R_1, R_2) = s_1 R_1 + s_2 R_2, \tag{3.39}$$

the Hamiltonian becomes

$$\begin{aligned}
K \;=\; & \frac{\kappa_1 \kappa_2}{2} \log\left(\frac{2G_1}{|\kappa_1|} + \frac{2s_2(G_2 - s_1 G_1)}{|\kappa_2|} \right. \\[2mm]
& \left. - \frac{4s_1 s_2}{\sqrt{|\kappa_1 \kappa_2|}} \sqrt{G_1 s_2(G_2 - s_1 G_1)} \cos Q_1 \right) \\[2mm]
& - \frac{\kappa_1^2}{2} \log\left(\frac{2G_1}{|\kappa_1|} - a^2 \right) - \frac{\kappa_2^2}{2} \log\left(\frac{2s_2(G_2 - s_1 G_1)}{|\kappa_2|} - a^2 \right) \\[2mm]
& + \frac{\kappa_1 \kappa_0}{2} \log\left(\frac{2G_1}{|\kappa_1|} \right) + \frac{\kappa_2 \kappa_0}{2} \log\left(\frac{2s_2(G_2 - s_1 G_1)}{|\kappa_2|} \right) \\[2mm]
& - \frac{\kappa_1 \kappa_2}{2} \log\left(\frac{4G_1 s_2(G_2 - s_1 G_1)}{|\kappa_1 \kappa_2|} \right. \\[2mm]
& \left. - \frac{4a^2 s_1 s_2}{\sqrt{|\kappa_1 \kappa_2|}} \sqrt{G_1 s_2(G_2 - s_1 G_1)} \cos Q_1 + a^4 \right),
\end{aligned} \tag{3.40}$$

and the corresponding motion equations are

$$\frac{\partial K}{\partial Q_1} = \frac{dG_1}{dt}, \quad \frac{\partial K}{\partial G_1} = -\frac{dQ_1}{dt} \tag{3.41}$$

$$\frac{\partial K}{\partial G_2} = -\frac{dQ_2}{dt}, \tag{3.42}$$

and the angular momentum becomes

$$
\begin{aligned}
I &= \kappa_1(x_{01}^2 + y_{01}^2) + \kappa_2(x_{02}^2 + y_{02}^2) \\[2mm]
&= \kappa_1\left(\frac{p_1^2 + q_1^2}{|\kappa_1|}\right) + \kappa_2\left(\frac{p_2^2 + q_2^2}{|\kappa_2|}\right) \\[2mm]
&= 2(s_1 R_1 + s_2 R_2) = 2G_2.
\end{aligned}
\tag{3.43}
$$

Since angular momentum is constant, Hamiltonian is cyclic in Q_2 and its conjugate G_2, which is angular momentum, is constant.

By employing these sets of canonical transformations we reduce the system from four-dimensional phase space to two-dimensional phase space with G_1 and Q_1. The ranges for the variables G_1, Q_1 and the constant G_2 are, $G_1 > \frac{a^2}{2}|\kappa_1|$, $G_2 > \frac{a^2}{2}(s_1|\kappa_1| + s_2|\kappa_2|)$ and $-2\pi < Q_1 < 2\pi$.

We consider a numerical example when $\kappa_1 = \kappa_2 = 1$ and $a = 1$. In this case the level curves of the Hamiltonian are shown in Figure 3.8 for $G_2 = 3$ in a coordinate system (X, Y), where $X = \sqrt{2R_1}\cos(P_1 - P_2)$ and $Y = \sqrt{2R_1}\sin(P_1 - P_2)$. That implies we are measuring the distance of the first vortex to the origin in the coordinate system (X, Y) that rotates with the second vortex.

In fact Figure 3.8 corresponds to the Poincare map in the system (p, q) where the angular momentum and the Hamiltonian are first integrals of motion. So the trajectories are plotted when the angular momentum and P_2 are fixed. We also notice that, in Figure 3.8, there are two fixed elliptic points at the points $(-\sqrt{3}, 0)$ and $(\sqrt{3}, 0)$ and that the trajectories are confined to the circles with radius 1 and $\sqrt{5}$. The inner circle in Figure 3.8 corresponds to the cylinder and the outer one exists since the total angular momentum is constant.

Figure 3.8. The level curves for the Hamiltonian in XY coordinates. Vortices have unit strength and there is no net circulation about the cylinder; $\kappa_0 = \kappa_1 + \kappa_2$. The coordinates of the points are: $A = (1.65, 0)$, $B = (1.322876, 0)$, $C = (1.2206, 0)$, $D = (1.15, 0)$, $E = (0, 1.5)$.

In Figure 3.9, the level curves of the Hamiltonian are shown for the case when vortices have opposite strengths. We see that when the initial position of vortices are close to the cylinder, they rotate around the cylinder. But when they start off far enough from the cylinder, they translate with uniform velocity (Figure 3.7).
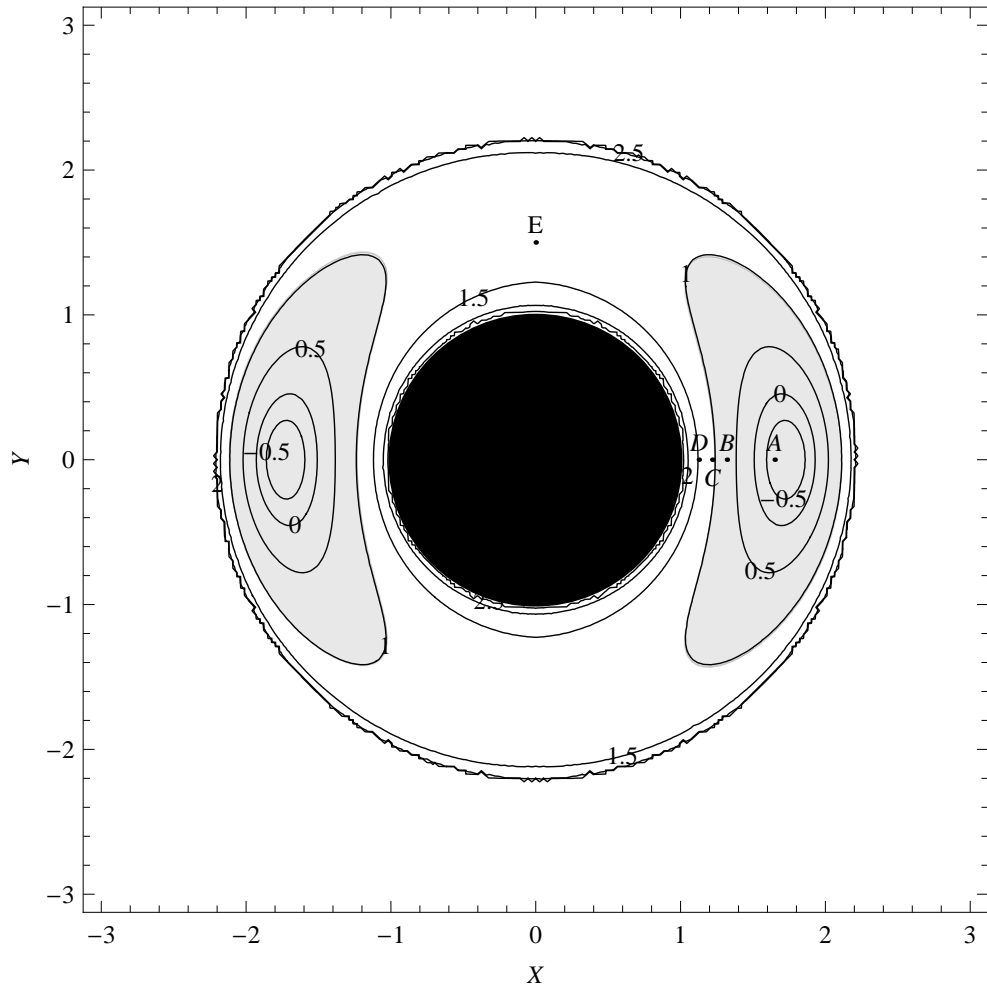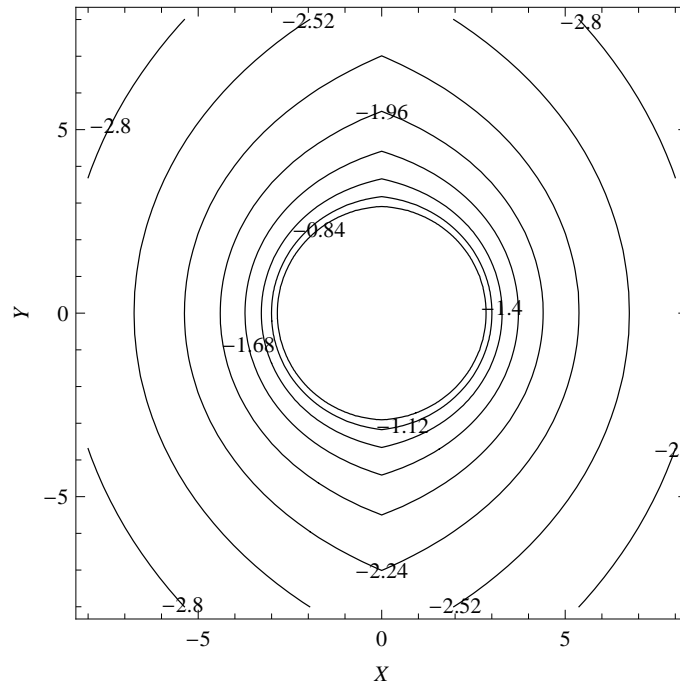

Figure 3.9. The level curves for the Hamiltonian in XY coordinates. Vortices have opposite unit strengths and there is no net circulation around the cylinder; $\kappa_0 = \kappa_1 + \kappa_2$.

3.2.4. Motion of Two Vortices around a Cylinder in the Presence of a Uniform Flow

Consider two vortices of strengths κ_1, κ_2 at z_{01}, z_{02}, a uniform flow with velocity along negative y axis u_0 and a cylinder of radius a at the origin. The complex potential is given by

$$\overline{V} = iu_0\left(1 + \frac{a^2}{z^2}\right) + \frac{i\kappa_1}{z - z_{01}} - \frac{i\kappa_1}{z - \frac{a^2}{\overline{z}_{01}}} + \frac{i\kappa_2}{z - z_{02}} - \frac{i\kappa_2}{z - \frac{a^2}{\overline{z}_{02}}} + \frac{i\kappa_0}{z} \qquad (3.44)$$

The motion of vortex at z_{01} can be found by

$$\frac{d\overline{z}_{01}}{dt} = iu_0\left(1 + \frac{a^2}{z_{01}}\right) + \frac{i\kappa_2}{z_{01} - z_{02}} - \frac{i\kappa_1\overline{z}_{01}}{|z_{01}|^2 - a^2} - \frac{i\kappa_2\overline{z}_{02}}{z_{01}\overline{z}_{02} - a^2} + \frac{i\kappa_0}{\overline{z}_{01}}. \qquad (3.45)$$

Similarly the motion of vortex at z_{02} can be found by

$$\frac{d\overline{z}_{02}}{dt} = iu_0\left(1 + \frac{a^2}{z_{02}}\right) + \frac{i\kappa_1}{z_{02} - z_{01}} - \frac{i\kappa_2\overline{z}_{02}}{|z_{02}|^2 - a^2} - \frac{i\kappa_1\overline{z}_{01}}{z_{02}\overline{z}_{01} - a^2} + \frac{i\kappa_0}{\overline{z}_{02}}. \qquad (3.46)$$

Letting $z_{01} = x_{01} + iy_{01}$ and $z_{02} = x_{02} + iy_{02}$ we have a system of four ordinary nonlinear differential equations

$$
\begin{aligned}
\frac{dx_{01}}{dt} &= \frac{2u_0a^2x_{01}y_{01}}{(x_{01}^2 + y_{01}^2)^2} + \frac{\kappa_2(y_{01} - y_{02})}{(x_{01} - x_{02})^2 + (y_{01} - y_{02})^2} - \frac{\kappa_1 y_{01}}{x_{01}^2 + y_{01}^2 - a^2} \\
&\quad + \frac{\kappa_0 y_{01}}{x_{01}^2 + y_{01}^2} + \frac{\kappa_2(a^2 y_{02} - y_{01}x_{02}^2 - y_{01}y_{02}^2)}{(a^2 - x_{01}x_{02} - y_{01}y_{02})^2 + (y_{01}x_{02} - x_{01}y_{02})^2} \\
&= \frac{2u_0a^2x_{01}y_{01}}{|z_{01}|^4} + \frac{\kappa_2(y_{01} - y_{02})}{|z_{01} - z_{02}|^2} - \frac{\kappa_1 y_{01}}{|z_{01}|^2 - a^2} + \frac{\kappa_0 y_{01}}{|z_{01}|^2} \\
&\quad + \frac{\kappa_2(a^2 y_{02} - y_{01}|z_{02}|^2)}{|z_{01}\overline{z}_{02} - a^2|^2}, \qquad (3.47)
\end{aligned}
$$

$$\frac{dy_{01}}{dt} = u_0 \left(\frac{a^2 y_{01}^2 - a^2 x_{01}^2}{(x_{01}^2 + y_{01}^2)^2} - 1 \right) - \frac{\kappa_2(x_{01} - x_{02})}{(x_{01} - x_{02})^2 + (y_{01} - y_{02})^2} - \frac{\kappa_0 x_{01}}{x_{01}^2 + y_{01}^2}$$

$$+ \frac{\kappa_1 x_{01}}{x_{01}^2 + y_{01}^2 - a^2} - \frac{\kappa_2(a^2 x_{02} - x_{01} y_{02}^2 - x_{01} x_{02}^2)}{(a^2 - x_{01} x_{02} - y_{01} y_{02})^2 + (y_{01} x_{02} - x_{01} y_{02})^2}$$

$$= u_0 \left(\frac{a^2 y_{01}^2 - a^2 x_{01}^2}{|z_{01}|^4} - 1 \right) - \frac{\kappa_2(x_{01} - x_{02})}{|z_{01} - z_{02}|^2} - \frac{\kappa_0 x_{01}}{|z_{01}|^2}$$

$$+ \frac{\kappa_1 x_{01}}{|z_{01}|^2 - a^2} - \frac{\kappa_2(a^2 x_{02} - x_{01} |z_{02}|^2)}{|z_{01} \overline{z}_{02} - a^2|^2}, \tag{3.48}$$

$$\frac{dx_{02}}{dt} = \frac{2u_0 a^2 x_{02} y_{02}}{(x_{02}^2 + y_{02}^2)^2} + \frac{\kappa_1(y_{02} - y_{01})}{(x_{02} - x_{01})^2 + (y_{02} - y_{01})^2} - \frac{\kappa_2 y_{02}}{x_{02}^2 + y_{02}^2 - a^2}$$

$$+ \frac{\kappa_0 y_{02}}{x_{02}^2 + y_{02}^2} + \frac{\kappa_1(a^2 y_{01} - y_{02} x_{01}^2 - y_{02} y_{01}^2)}{(a^2 - x_{02} x_{01} - y_{02} y_{01})^2 + (y_{02} x_{01} - x_{02} y_{01})^2}$$

$$= \frac{2u_0 a^2 x_{02} y_{02}}{|z_{02}|^4} + \frac{\kappa_1(y_{02} - y_{01})}{|z_{02} - z_{01}|^2} - \frac{\kappa_2 y_{02}}{|z_{02}|^2 - a^2} + \frac{\kappa_0 y_{02}}{|z_{02}|^2}$$

$$+ \frac{\kappa_1(a^2 y_{01} - y_{02} |z_{01}|^2)}{|z_{02} \overline{z}_{01} - a^2|^2}, \tag{3.49}$$

$$\frac{dy_{02}}{dt} = u_0 \left(\frac{a^2 y_{02}^2 - a^2 x_{02}^2}{(x_{02}^2 + y_{02}^2)^2} - 1 \right) - \frac{\kappa_1(x_{02} - x_{01})}{(x_{02} - x_{01})^2 + (y_{02} - y_{01})^2} - \frac{\kappa_0 x_{02}}{x_{02}^2 + y_{02}^2}$$

$$+ \frac{\kappa_2 x_{02}}{x_{02}^2 + y_{02}^2 - a^2} - \frac{\kappa_1(a^2 x_{01} - x_{02} y_{01}^2 - x_{02} x_{01}^2)}{(a^2 - x_{02} x_{01} - y_{02} y_{01})^2 + (y_{02} x_{01} - x_{02} y_{01})^2}$$

$$= u_0 \left(\frac{a^2 y_{02}^2 - a^2 x_{02}^2}{|z_{02}|^4} - 1 \right) - \frac{\kappa_1(x_{02} - x_{01})}{|z_{02} - z_{01}|^2} - \frac{\kappa_0 x_{02}}{|z_{02}|^2}$$

$$+ \frac{\kappa_2 x_{02}}{|z_{02}|^2 - a^2} - \frac{\kappa_1(a^2 x_{01} - x_{02} |z_{01}|^2)}{|z_{02} \overline{z}_{01} - a^2|^2}. \tag{3.50}$$

Consider the function

$$
\begin{aligned}
H &= u_0\kappa_1 x_{01}\left(1 - \frac{a^2}{x_{01}^2 + y_{01}^2}\right) + u_0\kappa_2 x_{02}\left(1 - \frac{a^2}{x_{02}^2 + y_{02}^2}\right) \\
&\quad + \frac{\kappa_1\kappa_2}{2}\log\left((x_{01} - x_{02})^2 + (y_{01} - y_{02})^2\right) \\
&\quad - \frac{\kappa_1^2}{2}\log\left(x_{01}^2 + y_{01}^2 - a^2\right) - \frac{\kappa_2^2}{2}\log\left(x_{02}^2 + y_{02}^2 - a^2\right) \\
&\quad + \frac{\kappa_1\kappa_0}{2}\log\left(x_{01}^2 + y_{01}^2\right) + \frac{\kappa_2\kappa_0}{2}\log\left(x_{02}^2 + y_{02}^2\right) \\
&\quad - \frac{\kappa_1\kappa_2}{2}\log\left((y_{01}x_{02} - x_{01}y_{02})^2 + (y_{01}y_{02} + x_{01}x_{02} - a^2)^2\right). \qquad (3.51)
\end{aligned}
$$

Then the motion equations become

$$
\frac{dx_{0i}}{dt} = \frac{1}{\kappa_i}\frac{\partial H}{\partial y_{0i}}, \quad \frac{dy_{0i}}{dt} = -\frac{1}{\kappa_i}\frac{\partial H}{\partial x_{0i}}, \quad i = 1, 2. \qquad (3.52)
$$

Hence the system is Hamiltonian. Consider the angular momentum

$$
I = \sum_{k=1}^{2}\kappa_k z_{0k}\overline{z}_{0k}. \qquad (3.53)
$$

Since

$$
\begin{aligned}
\frac{dI}{dt} &= \frac{d}{dt}\left(\sum_{k=1}^{2}\kappa_k z_{0k}\overline{z}_{0k}\right) \\
&= \kappa_1\left(2x_{01}\frac{dx_{01}}{dt} + 2y_{01}\frac{dy_{01}}{dt}\right) + \kappa_2\left(2x_{02}\frac{dx_{02}}{dt} + 2y_{02}\frac{dy_{02}}{dt}\right) \neq 0, \quad (3.54)
\end{aligned}
$$

angular momentum is not independent of time and hence the system is probably not integrable.

Consider the case $\kappa_1 = \kappa_2 = 1$, $\kappa_0 = 2$, $a = 1$, and $u_0 = 0.1$ then the motion of vortices starting at $z_{01} = 1.2206$ and $z_{02} = 2.1237$ (corresponding to point C of Figure
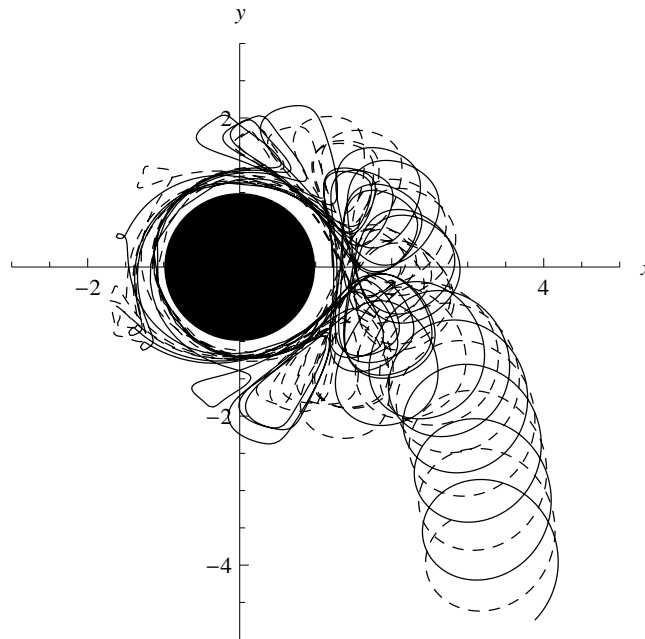
3.8) is shown in Figure 3.10.

Figure 3.10. Trajectories of two vortices in uniform flow $u_0 = 0.1$ with $\kappa_0 = \kappa_1 + \kappa_2$ and initial points $z_{01} = 1.2206$ and $z_{02} = 2.1237$. Continuous and dashed lines denote the trajectories of vortices. The initial points correspond to point C in Figure 3.8.

We can see that initially vortices rotate around the cylinder in a chaotic fashion and then escape to infinity. It can be shown that the trajectories depend on the initial conditions drastically, for example in Figure 3.11 initial conditions are $z_{01} = 1.322876$ and $z_{02} = 2.061553$ (corresponding to point B of Figure 3.8) and vortices rotate around the cylinder regularly as if there is no uniform flow (compare it with Figure 3.5). It is no coincidence that in the latter case initial points correspond to a region that is inside the grey shaded zone shown in Figure 3.8 and that in the former case we are just outside that zone.

A capture zone where vortices rotate around the cylinder is shown in Figure 3.8. Outside this zone, vortices escape to infinity unless they start off with initial points that correspond to points close to the cylinder in Figure 3.8, in which case they rotate around the cylinder just like the capture zone.

In fact, the choice of initial conditions are not arbitrary: for Figure 3.11 initial conditions are chosen such that we are inside the capture zone in Figure 3.8 (point B) and for Figure 3.10 initial conditions are chosen so that we are just outside the capture zone
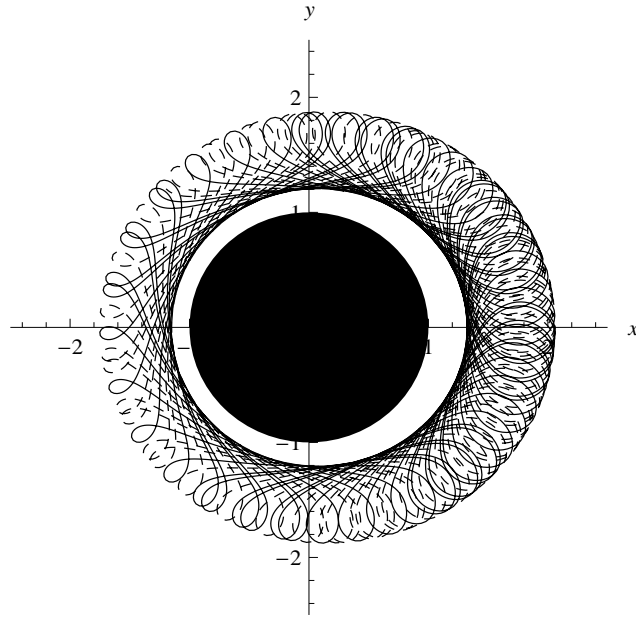
Figure 3.11. Trajectories of two vortices in uniform flow $u_0 = 0.1$ with $\kappa_0 = \kappa_1 + \kappa_2$ and initial points $z_{01} = 1.322876$ and $z_{02} = 2.061553$. Continuous and dashed lines denote the trajectories of vortices. The initial points correspond to point B in Fig. 3.8.

in Figure 3.8 (point C). So, we can conclude that if we are close enough to the elliptic point of the integrable case of two vortices without uniform flow, the trajectories in both cases would behave similarly (Figure 3.5 and Figure 3.11), but when we are far from the elliptic points (outside the capture zone), trajectories would behave differently (Figure 3.5 and Figure 3.10).

Point E of Figure 3.8 corresponds to the physical situation that vortices are placed such that the lines passing through the vortices and the origin are perpendicular. In this case vortices escape to infinity. Point A of Figure 3.8 is very close to the elliptic point and the initial positions of vortices are very close to eachother and the vortices rotate around the cylinder.

A Poincare section of the case with uniform flow would be helpful to analyze the system. Around the elliptical point we choose six different and arbitrary initial conditions and plot the position of the second vortex when the first vortex crosses the positive part of the x-axis (see Figure 3.12). For five initial conditions, the strobed trajectory points lie on invariant tori of the elliptical point (solid dots), while for the sixth initial condition, the points are scattered and eventually vortices escape to infinity (Figure 3.10).
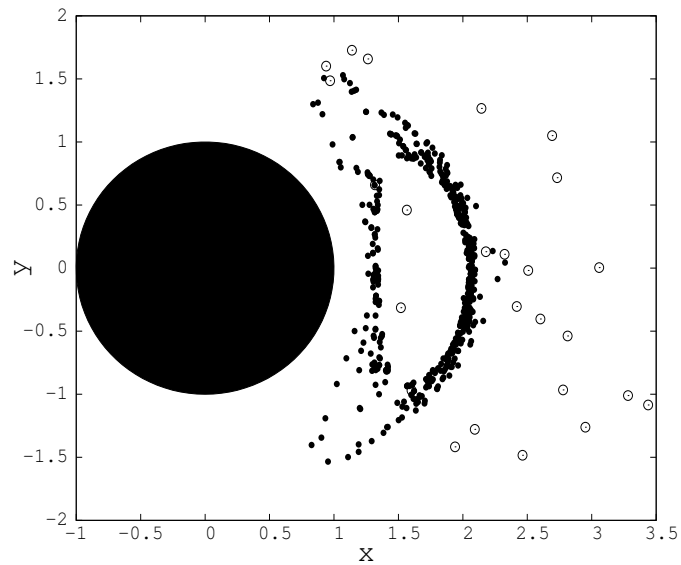
Figure 3.12. Poincare section for the parameters which generates the system of Fig. 3.10. Solid dots are used for the five different initial conditions for which the vortices lie on invariant tori of the elliptical point. Unfilled circles are used for the sixth initial condition that vortices eventually escape to infinity after several rotations around the cylinder.

In all numerical simulations, the Runge Kutta method with adaptive step size control is used to integrate the motion equations. Its results compare very well with the results of some standard packages. We notice that in almost all simulations involving chaotic behavior, it was necessary to vary the time step.

CHAPTER 4

OSCILLATING CYLINDER IN A UNIFORM FLOW WITH VORTICES

Oscillating cylinder problem with only one vortex has been solved (Kadtke & Novikov 1993). Here we shall consider the case of two vortices. We consider a cylinder of radius a at the origin interacting with two vortices which are placed at the points z_{01} and z_{02} with strengths of κ_1 and κ_2 in the presence of uniform flow. We add an oscillatory perturbation to the cylinder, chosen to move along the y-axis. We let frame of reference move with the cylinder so this perturbation results in a relative fluid velocity

$$u(t) = u_0(1 + \epsilon \sin \mathrm{w}t), \tag{4.1}$$

where $u(t)$ is the relative fluid velocity at infinity, w is the frequency and ϵ is the amplitude of the oscillation. (See Figure 4.1.)
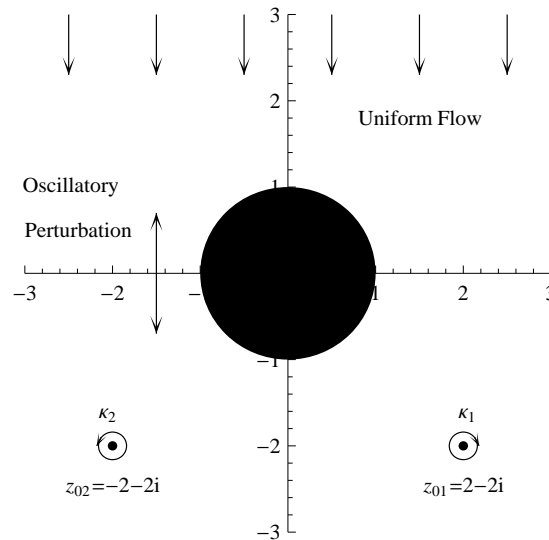

Figure 4.1. Diagram of the physical system represented by vortices-cylinder model, showing uniform flow field, two vortices placed at $z_{01} = 2 - 2i$ and $z_{02} = -2 - 2i$ with opposite strengths κ_1, κ_2, a cylinder with unit radius centred at the origin and direction of perturbation.

Then the complex potential, given by the equation (2.66), becomes

$$\overline{V} = iu_0(1 + \epsilon \sin \mathrm{w}t)\left(1 + \frac{a^2}{z^2}\right) + \frac{i\kappa_1}{z - z_{01}} - \frac{i\kappa_1}{z - \frac{a^2}{\overline{z}_{01}}} + \frac{i\kappa_2}{z - z_{02}} - \frac{i\kappa_2}{z - \frac{a^2}{\overline{z}_{02}}} + \frac{i\kappa_0}{z}.\,(4.2)$$

So the equations of motion of vortices and the Hamiltonian is slightly different from the previous case

$$
\begin{aligned}
\frac{dx_{01}}{dt} &= \frac{2u_0(1 + \epsilon \sin \mathrm{w}t)a^2 x_{01}y_{01}}{(x_{01}^2 + y_{01}^2)^2} + \frac{\kappa_2(y_{01} - y_{02})}{(x_{01} - x_{02})^2 + (y_{01} - y_{02})^2} - \frac{\kappa_1 y_{01}}{x_{01}^2 + y_{01}^2 - a^2} \\[2mm]
&\quad + \frac{\kappa_0 y_{01}}{x_{01}^2 + y_{01}^2} + \frac{\kappa_2(a^2 y_{02} - y_{01}x_{02}^2 - y_{01}y_{02}^2)}{(a^2 - x_{01}x_{02} - y_{01}y_{02})^2 + (y_{01}x_{02} - x_{01}y_{02})^2} \\[2mm]
&= \frac{2u_0(1 + \epsilon \sin \mathrm{w}t)a^2 x_{01}y_{01}}{|z_{01}|^4} + \frac{\kappa_2(y_{01} - y_{02})}{|z_{01} - z_{02}|^2} - \frac{\kappa_1 y_{01}}{|z_{01}|^2 - a^2} + \frac{\kappa_0 y_{01}}{|z_{01}|^2} \\[2mm]
&\quad + \frac{\kappa_2(a^2 y_{02} - y_{01}|z_{02}|^2)}{|z_{01}\overline{z}_{02} - a^2|^2},
\end{aligned}
\tag{4.3}
$$

$$
\begin{aligned}
\frac{dy_{01}}{dt} &= u_0(1 + \epsilon \sin \mathrm{w}t)\left(\frac{a^2 y_{01}^2 - a^2 x_{01}^2}{(x_{01}^2 + y_{01}^2)^2} - 1\right) - \frac{\kappa_2(x_{01} - x_{02})}{(x_{01} - x_{02})^2 + (y_{01} - y_{02})^2} \\[2mm]
&\quad - \frac{\kappa_0 x_{01}}{x_{01}^2 + y_{01}^2} + \frac{\kappa_1 x_{01}}{x_{01}^2 + y_{01}^2 - a^2} - \frac{\kappa_2(a^2 x_{02} - x_{01}y_{02}^2 - x_{01}x_{02}^2)}{(a^2 - x_{01}x_{02} - y_{01}y_{02})^2 + (y_{01}x_{02} - x_{01}y_{02})^2} \\[2mm]
&= u_0(1 + \epsilon \sin \mathrm{w}t)\left(\frac{a^2 y_{01}^2 - a^2 x_{01}^2}{|z_{01}|^4} - 1\right) - \frac{\kappa_2(x_{01} - x_{02})}{|z_{01} - z_{02}|^2} - \frac{\kappa_0 x_{01}}{|z_{01}|^2} \\[2mm]
&\quad + \frac{\kappa_1 x_{01}}{|z_{01}|^2 - a^2} - \frac{\kappa_2(a^2 x_{02} - x_{01}|z_{02}|^2)}{|z_{01}\overline{z}_{02} - a^2|^2},
\end{aligned}
\tag{4.4}
$$

62

$$\frac{dx_{02}}{dt} = \frac{2u_0(1 + \epsilon\sin \mathrm{w}t)x_{02}y_{02}}{(x_{02}^2 + y_{02}^2)^2} + \frac{\kappa_1(y_{02} - y_{01})}{(x_{02} - x_{01})^2 + (y_{02} - y_{01})^2} - \frac{\kappa_2 y_{02}}{x_{02}^2 + y_{02}^2 - a^2}$$

$$+ \frac{\kappa_0 y_{02}}{x_{02}^2 + y_{02}^2} + \frac{\kappa_1(a^2 y_{01} - y_{02}x_{01}^2 - y_{02}y_{01}^2)}{(a^2 - x_{02}x_{01} - y_{02}y_{01})^2 + (y_{02}x_{01} - x_{02}y_{01})^2}$$

$$= \frac{2u_0(1 + \epsilon\sin \mathrm{w}t)a^2 x_{02}y_{02}}{|z_{02}|^4} + \frac{\kappa_1(y_{02} - y_{01})}{|z_{02} - z_{01}|^2} - \frac{\kappa_2 y_{02}}{|z_{02}|^2 - a^2} + \frac{\kappa_0 y_{02}}{|z_{02}|^2}$$

$$+ \frac{\kappa_1(a^2 y_{01} - y_{02}|z_{01}|^2)}{|z_{02}\overline{z}_{01} - a^2|^2}, \tag{4.5}$$

$$\frac{dy_{02}}{dt} = u_0(1 + \epsilon\sin \mathrm{w}t)\left(\frac{a^2 y_{02}^2 - a^2 x_{02}^2}{(x_{02}^2 + y_{02}^2)^2} - 1\right) - \frac{\kappa_1(x_{02} - x_{01})}{(x_{02} - x_{01})^2 + (y_{02} - y_{01})^2}$$

$$+ \frac{\kappa_2 x_{02}}{x_{02}^2 + y_{02}^2 - a^2} - \frac{\kappa_0 x_{02}}{x_{02}^2 + y_{02}^2} - \frac{\kappa_1(a^2 x_{01} - x_{02}y_{01}^2 - x_{02}x_{01}^2)}{(a^2 - x_{02}x_{01} - y_{02}y_{01})^2 + (y_{02}x_{01} - x_{02}y_{01})^2}$$

$$= u_0(1 + \epsilon\sin \mathrm{w}t)\left(\frac{a^2 y_{02}^2 - a^2 x_{02}^2}{|z_{02}|^4} - 1\right) - \frac{\kappa_1(x_{02} - x_{01})}{|z_{02} - z_{01}|^2} - \frac{\kappa_0 x_{02}}{|z_{02}|^2}$$

$$+ \frac{\kappa_2 x_{02}}{|z_{02}|^2 - a^2} - \frac{\kappa_1(a^2 x_{01} - x_{02}|z_{01}|^2)}{|z_{02}\overline{z}_{01} - a^2|^2}, \tag{4.6}$$

$$H = u_0(1 + \epsilon\sin wt)\left(\kappa_1 x_{01}(1 - \frac{a^2}{x_{01}^2 + y_{01}^2}) + \kappa_2 x_{02}(1 - \frac{a^2}{x_{02}^2 + y_{02}^2})\right)$$

$$+ \frac{\kappa_1 \kappa_2}{2}\log\left((x_{01} - x_{02})^2 + (y_{01} - y_{02})^2\right)$$

$$- \frac{\kappa_1^2}{2}\log\left(x_{01}^2 + y_{01}^2 - a^2\right) - \frac{\kappa_2^2}{2}\log\left(x_{02}^2 + y_{02}^2 - a^2\right)$$

$$+ \frac{\kappa_1 \kappa_0}{2}\log\left(x_{01}^2 + y_{01}^2\right) + \frac{\kappa_2 \kappa_0}{2}\log\left(x_{02}^2 + y_{02}^2\right)$$

$$- \frac{\kappa_1 \kappa_2}{2}\log\left((y_{01}x_{02} - x_{01}y_{02})^2 + (y_{01}y_{02} + x_{01}x_{02} - a^2)^2\right). \tag{4.7}$$

The motion equations can be written down using

$$\frac{dx_{0i}}{dt} = \frac{1}{\kappa_i}\frac{\partial H}{\partial y_{0i}} , \quad \frac{dy_{0i}}{dt} = -\frac{1}{\kappa_i}\frac{\partial H}{\partial x_{0i}} , \quad i = 1, 2. \tag{4.8}$$

In Figures 4.2-4.4, trajectories of the vortices are shown for different initial conditions. For all cases, vortices' initial positions are on y axis: In Figure 4.2 vortices are on points $z_{01} = (0, 1.126865)$, $z_{02} = (0, 2.174897)$ (corresponding just to the right of point D of Figure 3.8) initially and both vortices escape to infinity eventually after both of them rotate around the cylinder many times.

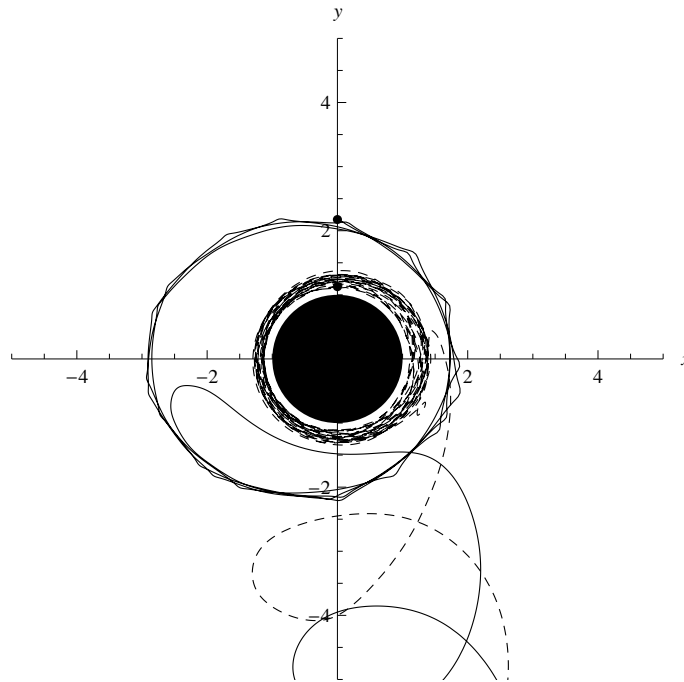Figure 4.2. Trajectories of two vortices. The parameters are $\kappa_1 = 1$, $\kappa_2 = 1$, $\kappa_0 = 2$, $\epsilon = 0.1$, w $= 1$, $u_0 = 0.1$, $z_{01} = (0, 1.126865)$, $z_{02} = (0, 2.174897)$. Continuous and dashed lines denote the trajectories of vortices. Initial points correspond to a point just to the right of point D of Fig. 3.8. Small solid dots indicate the initial positions of vortices.

For the second and third case (Figures 4.3 and 4.4) vortices start at points $z_{01} = (0, 1.126200)$, $z_{02} = (0, 2.175241)$ and $z_{01} = (0, 1.126200)$, $z_{02} = (0, 2.175241)$, respectively, and there is no escape to infinity. The choice of initial conditions are not arbitrary, they were chosen such that in Figure 3.8 we are close to the cylinder and away from the elliptic point. Initial points for Figure 4.3 correspond to point D of Figure 3.8 which is close to the cylinder, so vortices rotate around the cylinder. For Figure 4.4, initial points correspond to point C of Figure 3.8 and vortices rotate around the cylinder. So we conclude that if we are close enough to the cylinder (Figure 4.3) or to the capture zone (Figure 4.4), vortices rotate, however, if we are just in between these regions escape occurs (Figure 4.2). So the capture zone is roughly valid (slightly enlarged) for the case of vibrating cylinder.

Figure 4.3. Trajectories of two vortices. The parameters are $\kappa_1 = 1$, $\kappa_2 = 1$, $\kappa_0 = 2$, $\epsilon = 0.1$, w $= 1$, $u_0 = 0.1$, $z_{01} = (0, 1.126200)$, $z_{02} = (0, 2.175241)$. Continuous and dashed lines denote the trajectories of vortices. Initial points correspond to the point D of Fig. 3.8. Small solid dots indicate the initial positions of vortices.
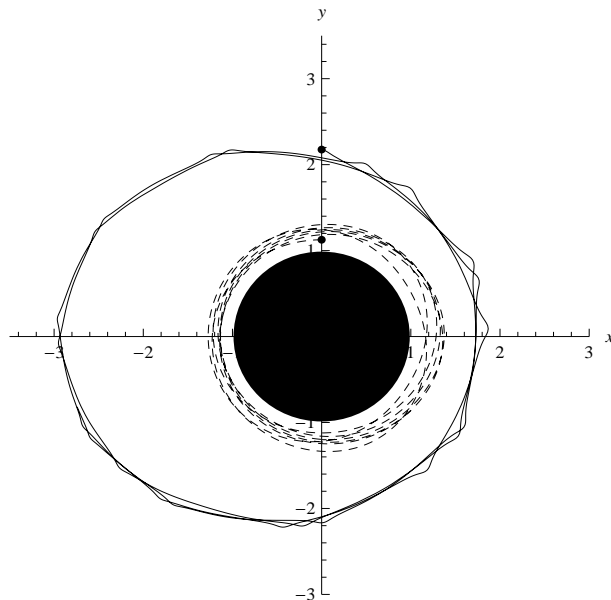
Figure 4.4. Trajectories of two vortices. The parameters are $\kappa_1 = 1$, $\kappa_2 = 1$, $\kappa_0 = 2$, $\epsilon = 0.1$, w $= 1$, $u_0 = 0.1$, $z_{01} = (0, 1.220600)$, $z_{02} = (0, 2.175241)$. Continuous and dashed lines denote the trajectories of vortices. Initial points correspond to the point C of Fig. 3.8. Small solid dots indicate the initial positions of vortices.
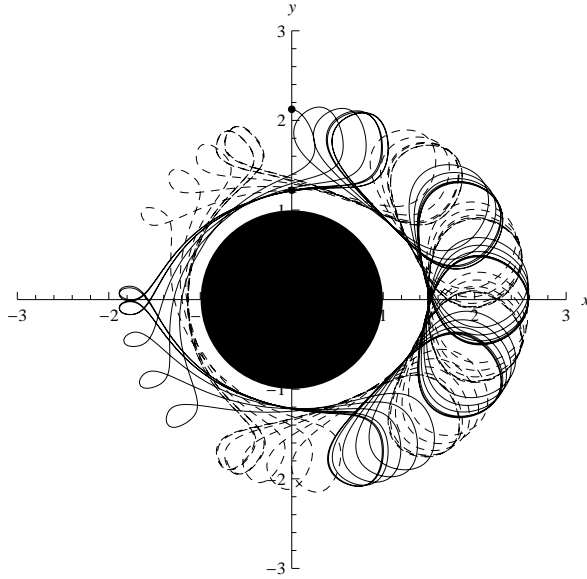
Chaotic interaction of a cylinder with vortices could result in large forces compared with the integrable case (Figures 4.5 and 4.6). Magnitude of the force on the cylinder in the integrable case of two vortices is shown in Figure 4.5. For chaotic cases when there is a uniform flow together with perturbation on the cylinder and two vortices (Figure 4.6), force on the cylinder is twice as large as the force in integrable case. This has physical applications such as the interaction of tethers of Tension Leg Platforms with vortices and uniform flow.
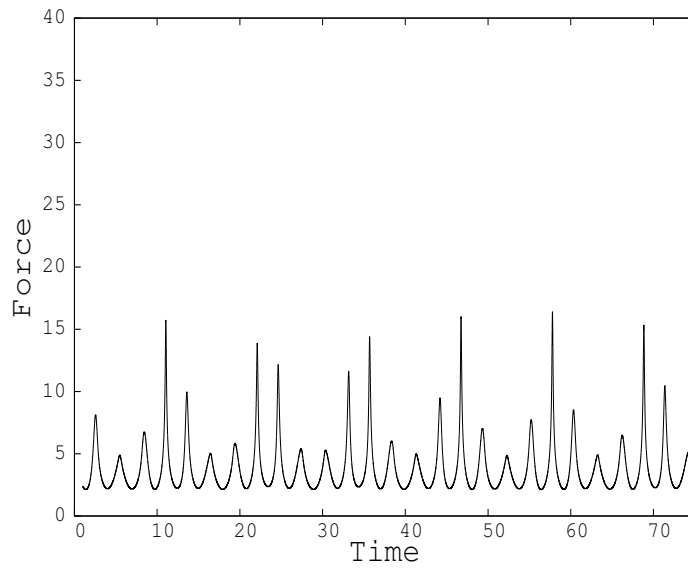
Figure 4.5. Magnitude of force on the cylinder. The parameters are $\kappa_1 = 1$, $\kappa_2 = 1$, $\kappa_0 = 2$, $u_0 = 0$, $z_{01} = 1.2206$, $z_{02} = 2.1237$.
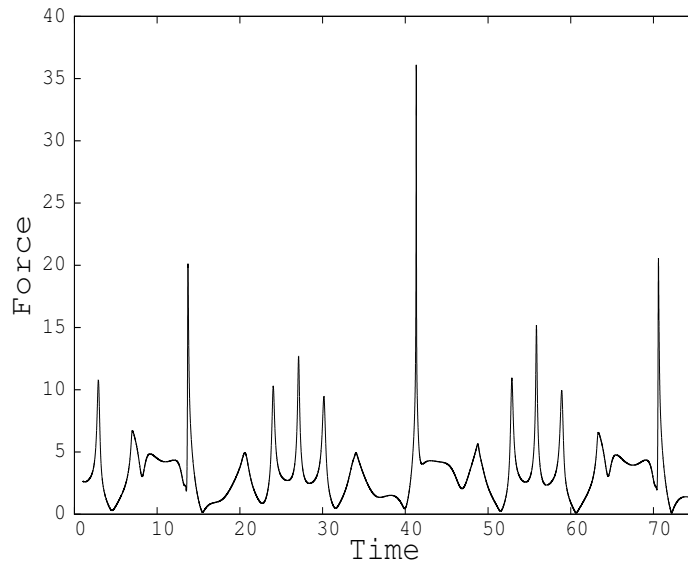

Figure 4.6. Magnitude of force on the cylinder. The parameters are $\kappa_1 = 1$, $\kappa_2 = 1$, $\kappa_0 = 2$, $\epsilon = 0.1$, $w = 1$, $u_0 = 0.1$, $z_{01} = 1.2206$, $z_{02} = 2.1237$.

CHAPTER 5

CONCLUSIONS

Problems considered in this thesis are, the problem of fluid advection excited by point vortices in the presence of stationary cylinders with and without uniform flow, the problem of motion of vortices around cylinders, the integrability of motion of the system of two vortices with one cylinder without uniform flow, and finally the problem of chaotic interaction of a cylinder with vortices by adding uniform flow to the system of two vortices with one cylinder and adding a perturbation to the cylinder.

For the first problem an analytical-numerical method has been developed, using complex analysis, to solve hydrodynamic interaction between an arbitrary number of cylinders and vortices. In the fluid advection problem forces are calculated. The arbitrary independent circulation around the cylinder, κ_0, is an important parameter in force calculations; for the case of vortices with opposite signs with or without uniform flow κ_0 must be zero for force to be zero.

For the second problem the Hamiltonian for the motion of vortices without uniform flow is constructed, reduced and constant Hamiltonian (energy) curves are plotted and the system is shown to be integrable according to Liouville. Motion of vortices with unit strength are confined to a region between two concentric circles; small circle representing the cylinder and the larger one exists due to the conservation of angular momentum (Figure 3.8). There are also two fixed elliptical points.

By adding uniform flow to the system the symmetry is destroyed and the system is no longer integrable (Figure 3.10). However by choosing the initial points close to the elliptic points of the integrable case in Figure 3.8, we are able to obtain trajectories confined to a thick orbit around the cylinder (Figure 3.11). A Poincare section analysis was useful to demonstrate that away from the elliptic points motions are chaotic (Figure 3.12).

Finally by allowing the cylinder to vibrate we model the natural vibration of the cylinder in the flow field, which has applications in ocean engineering involving tethers or pipelines in a flow field. Interesting cases of chaotic capture and escape are shown in Figures 4.1-4.3. We also observe that chaotic interaction may cause large forces on the cylinder depending on the initial positions of vortices (Figures 4.4 and 4.5).

There are similarities and differences between the one vortex case of (Kadtke

& Novikov 1993) and the present investigation of two vortices. In both cases, chaotic capture and escape of the vortex (vortices) occurs. Kadtke & Novikov gives a capture zone in Figure 12 of their paper, which is closely related to the separatrix. In the present case of two vortices, a capture zone plot similar to the one given by Kadtke & Novikov is given in Fig.3.8. When u_0 is small, say, less than 0.1, and there is no vibration, vortices with initial points corresponding to a region inside the capture zone will not escape to infinity (see Figure 3.11). So, for initial points corresponding to points that are inside the capture zone or that are close to the cylinder in Figure 3.8, vortices rotate around the cylinder. Outside these two regions, vortices escape to infinity.

When there is vibration of small magnitude, $\epsilon = 0.1$, and of frequency w $= 1$, the capture zone plot is still roughly valid (see Figures 4.1-4.3). For Figures 4.2 and 4.3, the initial points correspond to the points D and C of Figure 3.8 and there is no escape. However for Figure 4.1, the initial points are chosen to correspond just to the right of point D (between C and D) and vortices escape. We can conclude that the effect of perturbation is to enlarge the capture zone slightly.

REFERENCES

Aref, H. & Pomphrey, N. 1982 Integrable and chaotic motions of four vortices I. The case of identical vortices. *Proc. R. Soc. Lond. A* **380**, 359–387.

Aref, H., 1983: Integrable, chaotic, and turbulent vortex motion in two dimensional flows, *Ann. Rev. Fluid Mech.* **15**, 345–389.

Aref, H., Kadtke, J.B., Zawadzki, I., Campbell, L.J. & Eckhardt, B. 1987 Point vortex dynamics: Recent results and open problems. *Fluid Dyn. Res* **3**, 63.

Bagrets, A.A. & Bagrets, D.A. 1997 Nonintegrability of two problems in vortex dynamics. *Chaos* **7**, 368.

Banik, A.K. & Datta, T.K. 2009 Stability Analysis of TLP tethers under Vortex Induced Oscillations. *Journal of Offshore Mechanics and Arctic Engineering* **131**, 011601.

Burton, D.A., Gratus, J. & Tucker, R.W. 2004 Hydrodynamic forces on two moving discs. *Theoret. Appl. Mech.* **31**, 153–188.

Castilla, M.S.A.C., Moauro V., Negrini P. & Oliva, W.M 1993 The four positive vortices problem: regions of chaotic behaviour and the non-integrability. *Annales de l'I.H.P., section A,* tome **59**, no 1, 99–115.

Crowdy, D. and Marshall, J. 2005 The motion of a point vortex around multiple circular cylinders. *Phys. Fluids* **17**, 056602.

Dong, Y., Xie, G & Lou, J.Y.K. 1992 Stability of Vortex Induced Oscillations of Tension Leg Platforms. *Ocean Eng.* **19**, 555–571.

Eckhardt, B. 1988 Integrable four vortex motion. *Phys. Fluids* **31**, 2796–2801.

Eckhardt, B. & Aref, H. 1988 Integrable and chaotic motions of four vortices II. Collision dynamics of vortex pairs. *Phil. Trans. R. Soc. Lond. A* **326**, 655–696.

Helmholtz, H., 1858: Uber integrale hydrodinamischen gieichungen weiche den wirbelbewegungen entsprechen, *J. Reine Angew Math.*, **55**, 25.

Johnson, E.R. & McDonald, N.R. 2004 The Motion of a Vortex Near Two Circular Cylinders. *Proc. R. Soc. London A* **460**, 939–954.

Johnson, E.R. and McDonald, N.R. 2005 The point island approximation in vortex dynamics. *Geophysical and Astrophysical Fluid Dynamics* **99(1)**, 49–60.

Kadtke, J.B. & Novikov, E.A. 1993 Chaotic Capture of Vortices by a Moving Body I. Single Point Vortex Case. *Chaos* **3**, 543–553.

Kirchhoff, G., 1883: Vorlesungen Uber Matematische Physik, *Teubner, Leipzig*, Vol I.

Linton, C.M. & Evans, D.V. 1990 The Interaction of Waves with Arrays of Vertical Circular Cylinder. *J. Fluid Mech.* **215**, 549–69.

Maze, G., Carton, X. & Lapeyre, G. 2004 Dynamics of a 2D Vortex Doublet Under External Deformation. *Regular and Chaotic Dynamics*, **9(4)**, 477-497.

Meunier, P., Ehrenstein, U., Leweke, T. & Rossi, M. 2002 A merging criterion for two-dimensional co-rotating vortices. *Physics of Fluids*, **14(8)**, 2757-2767.

Milne-Thomson L M 1968 *Theoretical Hydrodynamics* London, Macmillan

Newton, Paul K. 2000 *The N-Vortex Problem: Analytical Techniques* Springer-Verlag New York, Inc.

Pashaev, O. & Yilmaz, O. 2008 Vortex Images and q-Elementary Functions. *Journal of Physics A-Mathematical and Theoretical*, **41**, 135207.

Pashaev, O. & Yilmaz, O. 2009 Power Series Solution for the Two Dimensional Inviscid Flow with a Vortex and Multiple Cylinders. *Journal of Engineering Mathematics*, **65**, 157.

Pashaev, O. & Yilmaz, O. 2010 Hamiltonian dynamics of N vortices in concentric annular region. *Journal of Physics A-Mathematical and Theoretical*, **44**, 185501.

Poincaré, H., 1893: Théorie des tourbillous, *Paris, Carré*, 205.

Tabor, M. 1989 *Chaos and Integrability in Nonlinear Dynamics: An Introduction* Wiley-Interscience, New York.

Tulu, S. & Yilmaz, O. 2010 Motion of Vortices Outside a Cylinder. *Chaos* **20**, 043103.

Williamson, C.H.K. & Govardhan, R. 2004 Vortex Induced Vibrations. *Annu. Rev. Fluid Mech.* **36**, 413–55.

Yilmaz, O. 1998 Hydrodynamic Interactions of Waves with a Group of Truncated Vertical Cylinders. *Journal of Waterway, Port, Coastal & Ocean Engineering* **124**, 272-279.

Zannetti & Franzese, P. 1993 Advection by a point vortex in closed domains. *Eur. J. Mech., B/Fluids*, **12**, 43–67.

Ziglin, S. L. 1980: Nonintegrability of a problem on the motion of four point vortices, *Dokl. AN SSSR* **250**, 1296.

Ziglin, S. L. 1983: The nonintegrability of the problem of the motion of four vortices of finite strengths, *Physica D* **4**, 268.

VITA

Date of Birth and Place: 26.10.1980, İzmir – Turkey

EDUCATION

2007- 2011 Doctor of Philosophy in Mathematics
Graduate School of Engineering and Sciences, İzmir Institute of Technology,
İzmir - Turkey
Thesis Title: "Vortex Dynamics in Domains with Boundaries"
Supervisor: Prof. Dr. Oğuz Yılmaz

2003 - 2005 Master of Science in Mathematics
Institute of Engineering and Science, Bilkent University,
Ankara - Turkey
Thesis Title: "Limiting Gibbs Measures in Some One and Two Dimensional Models"
Supervisor: Prof. Dr. Azer Kerimov

1998 - 2003 Bachelor of Mathematics
Department of Mathematics, Dokuz Eylül University, İzmir - Turkey

PROFESSIONAL EXPERIENCE

2003 - 2005 Research and Teaching Assistant
Department of Mathematics, Bilkent University,
Ankara – Turkey

PUBLICATIONS

Kaptanoğlu, H. T. and Tülü, S*., "Weighted Bloch, Lipschitz, Zygmund, Bers, and Growth Spaces of the Ball: Bergman Projections and Characterizations"*, Taiwanese J. Math. 15 (2011), 101-127.

Tülü, S. and Yilmaz, O. *"Motion of Vortices Outside a Cylinder"* , Chaos 20 (2010), 043103.

e-mail: tuluserdar@gmail.com, serdartulu@iyte.edu.tr